University College of Southeast Norway

www.usn.no

FMH606 Master's Thesis 2017

Process Technology

Near-well simulations and modelling of oil production from reservoir

Ramesh Timsina

Faculty of Technology, Natural sciences and Maritime Sciences

Campus Porsgrunn

University College of Southeast Norway

www.usn.no

Course: FMH606 Master's Thesis, 2017

Title: Near-well simulations and modelling of oil production from reservoir

Number of pages: 64

Keywords: light oil production, inflow control devices, Oil and gas, water breakthrough, OLGA, Rocx, near well simulation

Student: Ramesh Timsina

Supervisor: Britt M. E. Moldestad

External partner: Acona Flow Technology

Availability: Open

Approved for archiving: _____

(supervisor signature)

Summary:

One of the major challenges that the oil industry faces today is water breakthrough and high production of water from mature oil fields. Early water breakthrough can occur due to high frictional pressure drop in the well or due to fractures in the reservoirs.

Conventional inflow control devices (ICDs) are designed to delay water breakthrough but do not have the capability to control the water inflow after breakthrough. Autonomous inflow control devices (AICDs) are developed to choke the inflow of water after breakthrough has occurred.

An integrated transient wellbore-reservoir model is developed in OLGA-Rocx and simulations are carried out with different types of inflow controllers. The functionality of the inflow controllers is studied for light oil reservoir and the results are compared. Additional simulations are carried out with heavy oil. Simulations are performed for different permeability profiles in the reservoir. The study includes fractured reservoir, heterogeneous reservoir and the homogeneous reservoir. The results show that autonomous inflow controllers have a higher potential to limit the water influx compared to the conventional ICDs.

In the homogeneous reservoir, the frictional pressure drop along the well was rather low causing similar production throughout the wellbore. Hence, the benefit of using AICDs was less significant than in the heterogeneous reservoir.

An equivalent AICD was chosen to represent eight normal AICDs to make the simulation more efficient in terms of both time and computational resources. Additional simulations were performed by using normal sized AICDs, and the results show that the accumulated oil was highly increased compared to the results obtained using the equivalent AICDs.

Preface

This study is the result of the research work carried out during Spring 2017 at University college of Southeast Norway with Acona Flow Technology as an external partner. This work is submitted in partial fulfillment of the requirements for the Master of Science Degree at University college of southeast Norway, Porsgrunn.

It covers the near well simulations of production from oil reservoirs. The functionality of conventional ICDs and AICDs were studied and compared for different reservoir/oil conditions.

Firstly, I would like to thank both the university college and Acona Flow Technology for granting me the opportunity to work on this thesis. I would like to thank my supervisor Prof. Britt M. E. Moldestad and my co-supervisors Rune Killie and Nora C.I. Furuvik, for their continuous guidance, support, encouragement and keeping patience throughout the period of this task. It is great pleasure to work with such persons with a wide spectrum of petroleum engineering experience and knowledge.

I would also like to thank the library staff and the IT staff of the university college of Southeast Norway for providing the various supports whenever required.

Finally, I would like to express gratitude for all the people close to me for their continuous support and motivation to give my best efforts for completing this work.

Porsgrunn, 15th May 2017

Ramesh Timsina

Nomenclature

Letters and expressions

a	Large half-axis of the drainage	m
A	(Cross sectional) area	m^2
B	Oil formation volume factor	-
C	Geometrical constant	-
D	Pipe diameter	m
F	Force	N
h	(Reservoir) height	m
I_{ani}	Vertical-to-horizontal permeability anisotropy	-
K	Absolute permeability	mD
K_H	Permeability in horizontal direction	mD
K_i	Effective permeability	mD
K_{ri}	Relative permeability of specific fluid phase	-
K_V	Permeability in vertical direction	mD
L	(Pipe) length	m
M	Mobility ratio	-
M_o	Molecular weight of oil	kmol/kg
P_1	Pressure of main flow upstream of valve	Pa
P_2	Pressure in pilot flow between laminar and turbulent flow element	Pa
P_3	Pressure of main flow downstream of valve	Pa
P_b	Bubble point pressure	Pa
p_f	Bubble point pressure factor	-
q	Fluid flow rate	m^3/s
Q_g	Volumetric flow rate of gas	m^3/s
Q_l	Volumetric flow rate of liquid	m^3/s
Q_o	Volumetric flow rate of oil	m^3/s
Q_w	Volumetric flow rate of water	m^3/s
r	Radius from center axis	m
r_e	Drainage radius	m

R_{sb}	Solution gas ratio at bubble point	scf/STB
r_w	Wellbore radius	m
SG	Specific gravity	-
T	Fluid temperature	K
v	Fluid velocity	m/s
x	Length	m
y_g	Mole fraction of gas	-
γ_g	Specific gravity of gas	-
γ_o	Specific gravity of oil	-
μ	Viscosity	cP
μ_i	Viscosity of specific fluid phase	cP
Φ	Porosity	-
π	Constant	-
ρ	Fluid density	Kg/m^3

Abbreviations

AICD	Autonomous Inflow Control Device
API	American Petroleum Institute
GLR	Gas Liquid Ratio
GOR	Gas Oil Ratio
GUI	Graphical User Interface
ICDs	Inflow Control Devices
ICV	Inflow Control Valve
scf	standard cubic foot
STB	Stock Tank Barrel
WC	Water Cut
WTI	West Texas Intermediate

Overview of tables and figures

List of Tables

List of Figures

Contents

1 Introduction

This thesis focuses on near-well simulation and modelling of oil production from a light oil reservoir. The phenomenon with which fluids enters the wellbore is crucial for effective and economical production. So, these systems must be designed in accordance with the physical behavior of the well completion. One of the major challenges that the oil industry faces today is early water breakthrough and high production of water from mature oil fields. Early water breakthrough can occur due to high frictional pressure drop in the well or due to fractures in the reservoirs. This causes reduction of the oil production and increases corrosion rates. In fact, some of the wells are shut down because of excessive water production. Oils with high water content require large separation systems, increasing both capital and operating cost for the plant. There have been several studies of this behavior and several types of devices have been developed to counteract this problem. There are different types of inflow control devices (ICDs) developed for delaying breakthrough of water and gas. They are designed to improve completion performance, the overall efficiency and the lifetime of the oil production.

Conventional ICDs are designed to delay water or gas breakthrough but do not have the capability to control the water inflow after breakthrough. So, there is no solution other than to choke the entire flow from the system after a certain point of time. Hence, there has been various development in this inflow control technologies with the autonomous operation. Autonomous inflow control device (AICD) chokes the fluid flow into the wellbore from the high permeable zone after the water breakthrough, allowing normal oil production from the other zones. This will enhance the well performance and increases the recovery of oil from existing reservoirs.

The oil reservoirs will show different behaviors at different conditions and this will affect the well performance. The integrated transient wellbore-reservoir model is developed in OLGA-Rocx GUI environment and simulations are carried out with different types of inflow controllers. The functionality of the inflow controllers for light and heavy oil reservoir is studied. It provides the general trends about the oil production and the different aspects associated with it.

1.1 Background of the study

The near well simulation of oil production from a heavy oil reservoir have been previously performed for different ICDs [1]. In this task, the near well simulation of oil production from a light oil reservoir with different ICDs are focused. Light crude oil production is the most economical and is currently serving as benchmark together with medium crude oil. The most of the conventional oil fields in the worlds are either light or medium crude oil. The major disadvantage with heavy oil production is transportation, due to its high viscosity and the refine costs. Extra costs will be added to make the heavy oil viable[2]. It is also important to optimize the oil production and recovery from light oil reservoirs.

Light oil has low viscosity, low specific gravity and high API gravity with a high amount of light hydrocarbons. They have higher commodity value as the light hydrocarbons fuels serves nearly the entire demand of fuel energy. Efficient production of light oil is essential for the economic benefits of the company.

Light oils have higher mobility and it is easier to extract more oil from these types of reservoirs. Generally, a long horizontal well has been used, to maximize the contact with the oil reservoir. This also enforces a proper design of near the well and the completion system. Hence, near well modelling and simulation is an important aspect of the oil industry.

1.2 Objective

The main objective of this work is to perform near well simulations of oil production from light oil reservoir using different types of ICDs with water drive. The simulations are performed based on integrated transient wellbore-reservoir model developed in OLGA-Rocx. The functionality of conventional ICDs and autonomous inflow controllers are studied and compared for different reservoir and oil conditions.

2 Literature review

This chapter gives the information about the light oil. Further, it gives an introduction to the components and technology that are used in oil production.

2.1 Light oil

In general, the crude oil is classified based on the density of hydrocarbon present in the oil and its ability to flow. This is characterized by API gravity of oil, which is given by Equation 2.1.

$$\text{API} = \frac{141.5}{\text{SG}} - 131.5 \tag{2.1}$$

Where SG is the specific gravity, which is the ratio of the density of oil to the density of water. The API gravity and the general viscosity range are given in Table 2-1 [3].

Table 2-1: Oil characterization based on API gravity and viscosity [3]

Oil Category	API Gravity	Viscosity
Light Oil	> 31.1°	< 100 cP
Medium Oil	22.3 – 31.1°	-
Heavy Oil	> 22.3°	> 100 cP
Extra heavy Oil	< 10°	-
Natural Bitumen	-	> 10000 cP

Presently, the conventional oil, which is referred to as light or medium oil is the benchmark of the crude oil. The crude like West Texas Intermediate (WTI) (API = 39.6), brent crude (API = 38.06) and Dubai crude (API = 31) serves as the benchmark crude across the globe. The light crude oil has low viscosity and flows freely at room temperature. It has low specific gravity because of low density and hence, Equation 2.1 gives a high API index. Light crude oils also have low wax content [4].

In most of the reservoirs, oil lies in contact with water and/or gas. As water and/or gas have lower viscosities, the mobility will be higher. This causes water/gas breakthrough at some point in time during oil production. In horizontal wells, the frictional losses increase with an increase in the well length. This, in turn, results in a higher drawdown pressure across the heel sections than in toe section which causes higher production rates in heel segment than in toe segment. Hence, the early water breakthrough occurs from the heel section in a homogeneous reservoir and causes uneven sweeping of drainage area. Also, a long wellbore is likely to encounter fractures in the reservoir. This heterogeneity causes an uneven influx to the wellbore. To overcome this problem, inflow control devices are installed along the entire well to obtain even distribution of inflow [5].

2.2 Inflow control technologies

An ICD is a well completion device used to choke the fluid flow entering base pipe from the annulus. It is a passive inflow control device, i.e. it does not have any active parts, which can be controlled or modified to regulate the flow through it. ICD adds up an additional pressure drop across the completion and restricts the inflow along the well. Generally, all the ICDs are self-operating in nature, as the settings cannot be changed after installation [6].

The higher flow rates from the high permeability zones cause early water breakthrough. The early water breakthrough can be delayed by having a higher flow restriction in high permeable zones. Further, ICD can produce at high rates from zones that have poorer production rate. This will increase the production and recovery.

The common types of ICDs present in the industry use either friction or restriction to create a pressure drop across it. The most commonly used ICDs are as follows:

- Channel type ICD
- Orifice/nozzle type ICD

Figure 2-1 shows the schematics of the channel type ICD that uses surface friction to develop the desired pressure drop. The fluid passes through a multi-layered screen into the annulus and enters the wellbore through the channels. The fluid is forced to change its flow direction several times, causing a pressure drop across it. The chances of erosion and plugging are low because of low fluid velocity. Channel ICDs are dependent on fluid viscosity. So, a large difference in oil and water viscosity after water breakthrough can cause non-uniform inflow to the wellbore [5].

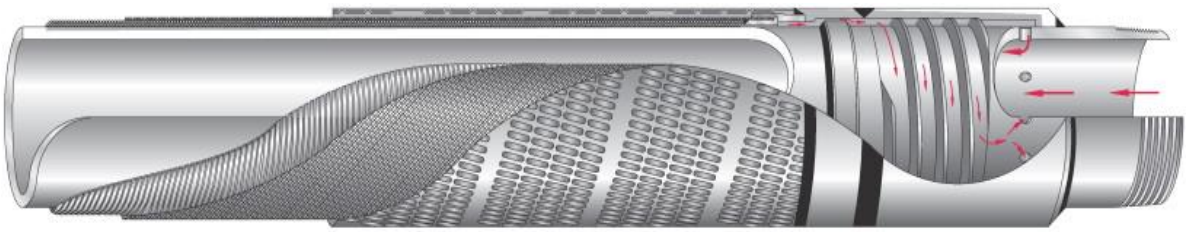

Figure 2-1: Channel ICD schematics [7]

Figure 2-2 shows the schematics of the orifice types of ICD that uses restriction of fluid flow to develop the desired pressure drop. Orifice ICDs are simple in design where the fluid passes through small diameter nozzles or orifices that create resistance. The pressure drop across the orifice ICD is instantaneous and is highly dependent on the density and velocity of the fluid. So, an orifice ICD is likely to have high sand erosion rate.

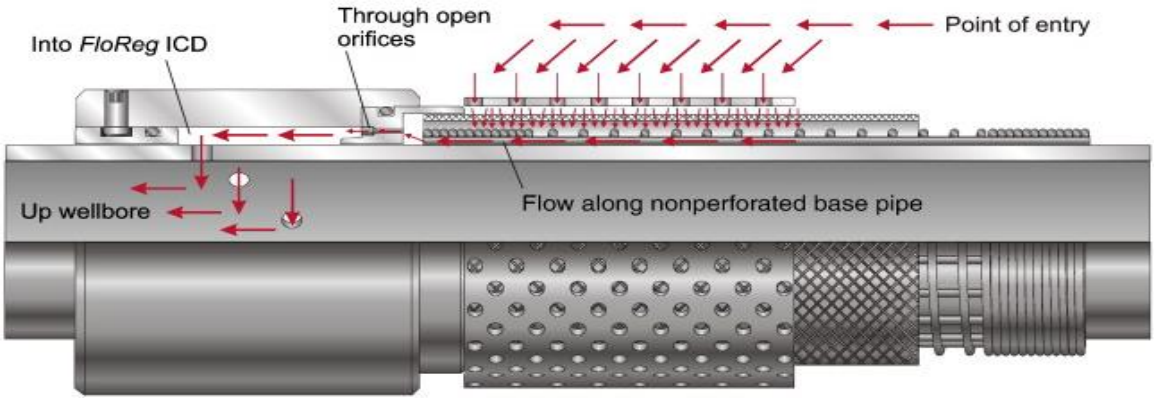

Figure 2-2: Orifice ICD schematics[7]

The pressure drop across an orifice can be expressed by:

$$\Delta P = C \cdot \frac{1}{2} \cdot \rho \cdot v^2 \tag{2.2}$$

Where, C is the geometrical constant, ρ is the fluid density and v is the fluid velocity. This types of ICD in not dependent on fluid viscosity, thus ideal for applications where viscosity sensitivity is low [5].

According to Fernandes et al., an ICD can work effectively when the frictional pressure drop across the wellbore is relatively high compared to the drawdown pressure. Fractured reservoir with long wells also favors the ICDs installations [5].

ICD is a passive device and cannot choke for water or gas breakthrough occurs. The oil industry has therefore focused on developing new technology for choking of such unwanted fluids. Inflow control valves (ICVs) are the example of this development. ICVs are active sliding sleeve valves, operated remotely by means of a controlling system. The electrical connection to the control room favors only for short wells. But the unpredicted reservoir behavior favors ICVs for higher recovery compared to ICDs. ICVs have flexible operation with the change in the operating conditions. ICVs are more expensive than ICDs as they have moving parts. ICDs are simple and have low installation risks as they don't have any moving parts, [8].

There has been new development on these ICVs to adjust the inflow automatically. Autonomous technology can adjust their performance based on the wellbore dynamics. Autonomous inflow controllers are being developed by companies like Halliburton, Statoil. The autonomous inflow control device developed by Statoil is called Rate Controlled Production (RCP) valves that choke low viscous fluid, allowing only high viscous fluid to flow through it [9].

3 Theoretical background

This chapter contains the basic theory associated with oil production from a reservoir. The different reservoir and fluid properties are presented below.

3.1 Reservoir Properties

3.1.1 Porosity

Porosity (Φ) is the storage capacity of the rock or the pore volume that is available for fluids. The porosity is given by Equation 3.1, expressed as the pore volume in the percentage of total volume of rock.

$$\Phi = \frac{\text{Total pore volume}}{\text{Total rock volume}} \times 100\% \tag{3.1}$$

Figure 3-1 illustrates the different types of porosity. Catenary pores and cul-de-sac pores account for effective porosity whereas closed pores account for ineffective porosity [10].

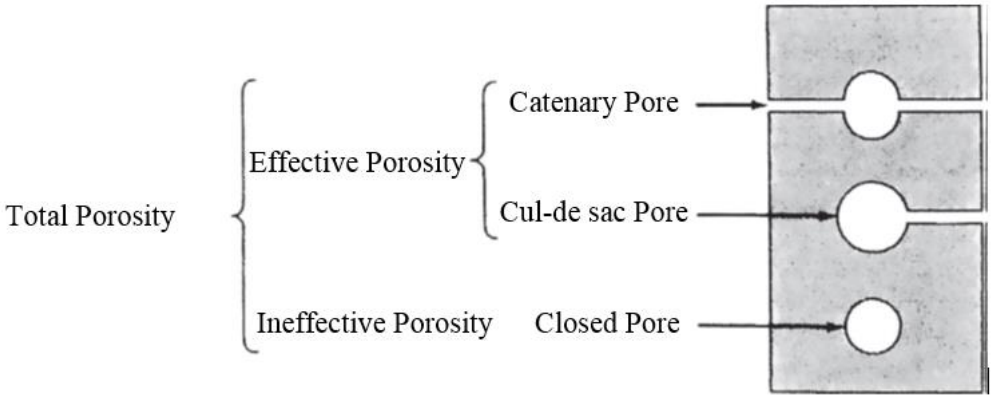

Figure 3-1: Classification of different types of porosity [10]

3.1.2 Permeability

Permeability is the ability of fluids to flow through the interconnected pores of the reservoir. Permeability is a dynamic property of the reservoir as it varies within the reservoir. Figure 3-2 shows the fluid flow and the rock permeability where the fluids can flow between the interconnected pores, but not in the isolated pores.

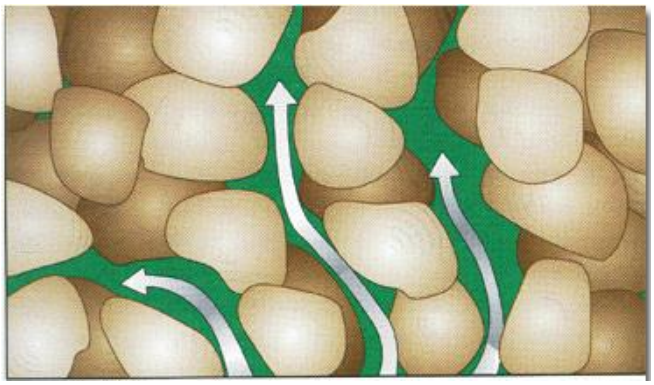

Figure 3-2: Fluid flow and rock permeability[11]

The rock permeability is an important rock property in addition to porosity, as it controls the movement, direction and the flow rates of fluids in the reservoir.

3.1.2.1 Relative permeability

The relative permeability has a significant effect on the potential of oil production from a reservoir. The relative permeability is defined as the ratio of the effective permeability to the absolute permeability.

$$K_{ri} = \frac{K_i}{K} \tag{3.2}$$

Where K_{ri} is the relative permeability of the specific fluid phase i, K_i is the effective permeability and K is the absolute permeability.

3.1.2.2 Darcy's law.

The fundamentals physics beyond rock permeability is complex. The Darcy's law gives the idea of fluid flow inside a reservoir. The general expression for Darcy's law is presented by:

$$q = -\frac{k}{\mu} \cdot A \cdot \frac{\Delta P}{\Delta x} \tag{3.3}$$

Where k is the absolute permeability, q is the volumetric flow rate of the fluid, A is the cross-sectional area, μ is the fluid viscosity and $\frac{\Delta P}{\Delta x}$ is the pressure drop per unit length.

Figure 3-3 represents a horizontal well with its axis along the x-direction. Hence, the fluid flow from the reservoir towards the well is radial.

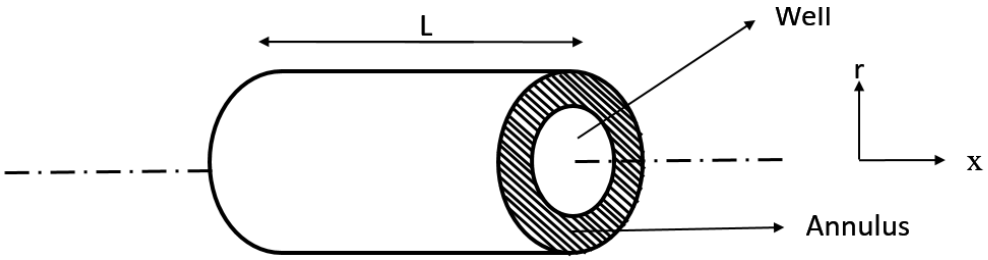

Figure 3-3: Horizontal well

Therefore, Darcy's law for the cylindrical coordinate system is given by the Equation 3.4.

$$q = -\frac{k}{\mu} \cdot A \cdot \frac{dP}{dr} \tag{3.4}$$

Where A is the radial flow surface area at a distance r from the axis of the well, given by Equation 3.5.

$$A = 2\pi r L \tag{3.5}$$

The driving force for the oil from the reservoir to the well is the pressure difference. According to Equation 3.4, the flow will increase with the increase of absolute permeability of the reservoir and the pressure drop. Generally, the vertical permeability differs from horizontal permeability in a reservoir. This difference causes an ellipsoidal drainage around the well. This permeability anisotropy is illustrated in Figure 3-4.

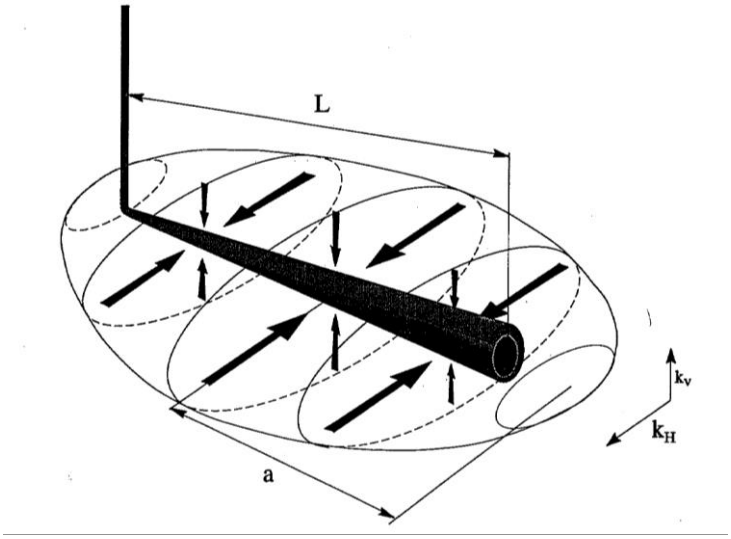

Figure 3-4: Drainage pattern formed around horizontal well [12]

According to Economides et al., a horizontal well deliverability relationship (mixed steady state in a horizontal plane and pseudo-steady state in the vertical plane) is given by Equation 3.6 [12].

$$q = \frac{k_H h \Delta p}{141.2 \cdot B \cdot \mu \left(\ln \left\{ \frac{\left[a + \sqrt{a^2 - (L/2)^2} \right]}{L/2} \right\} + \left(\frac{I_{ani} h}{L} \right) \ln \frac{I_{ani} h}{\left[r_w (I_{ani} + 1) \right]} \right)} \tag{3.6}$$

Where, q is the flow rate, k_H is the horizontal permeability, h is the reservoir height, Δp is pressure difference, B is the oil formation volume factor, μ is the fluid viscosity, L is the well length, r_w is the wellbore radius, r_e is the drainage radius, I_{ani} is the vertical-to-horizontal permeability anisotropy and is given by the Equation 3.7 [12].

$$I_{ani} = \sqrt{\frac{K_H}{K_V}} \tag{3.7}$$

a is the large half-axis of the ellipsoidal drainage and is given by the Equation 3.8 [12].

$$a = \frac{L}{2}\left\{0.5 + \left[0.25 + \left(\frac{r_e H}{L/2}\right)^4\right]^{0.5}\right\}^{0.5} \quad \text{for} \quad \frac{L}{2} < 0.9 r_e H \tag{3.8}$$

3.1.3 Water-drive reservoir

In water-drive reservoirs, the oil zone is in contact with the water layer (aquifer). This provides a force to act on the oil zone and makes the oil flow towards the wellbore. The main problems with the bottom water drive are the water-coning which can result in reduced oil production [13]. Figure 3-5 shows the overview of water drive inside a reservoir. Generally, water lies at the bottom due to its high density and provides extra pressure to the oil zone. The reservoir pressure decreases with time and hence the aquifer expands. The water moves towards the produced oil zone and maintains the reservoir pressure. The water-drive reservoir can have early water breakthrough.

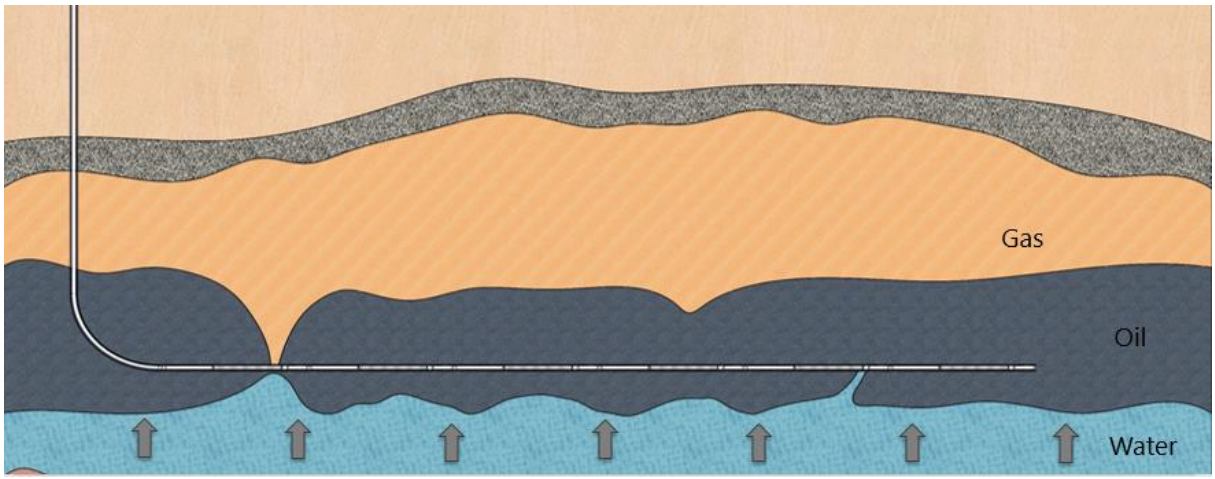

Figure 3-5: Horizontal well with water aquifer [14]

3.2 Fluid properties

It is essential to know the Pressure Volume Temperature (PVT) relation of the fluids that is being used in simulations. One of the models used to estimate the PVT relations is the black oil fluid model. The black oil fluid model is a model that assumes the oil components will always be in the liquid phase and does not evaporate at any conditions. Figure 3-6 shows the typical pressure-temperature phase diagram for ordinary black oil. This is characterized by approximately equally distributed quality lines. Quality lines are the lines showing the states of black oil at particular temperature and pressure. Liquid starts to shrink at a constant rate with the reduction of pressure along the path EF [15].

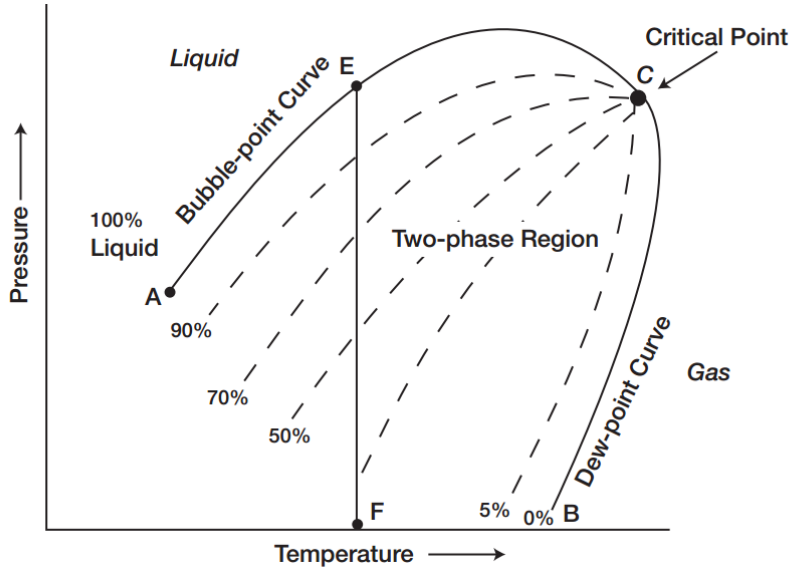

Figure 3-6: A typical p-T diagram for an ordinary black oil [15]

3.2.1 GOR model- Lasater correlation

In 1958, Lasater developed a bubble point pressure correlation based on experimentally measured data for the different crude oils across Canada, and US [16]. Lasater purposed a unique "effective oil molecular weight" to a given black oil sample. The author defined different variables to specify the PVT relation of that crude. The relation was developed based on the two charts that were developed by Lasater [17]. The developed relations are presented in Appendix B: Lasater correlation. This correlation can be applied in the range of 17.9° < API < 51.1°. The range of data used to develop this Lasater correlation is presented in Table 3-1 [17].

Table 3-1: Data range used in lasater correlation

Range	Units
$3.309 < P_b < 398.517$	bar
$27.78 < T < 1\ 33.33$	°C
$3 < R_{sb} < 2905$	scf/STB
$17.9° < API < 51.1°$	°API
$0.574 < \gamma_g < 1.223$	(air = 1)

Where P_b is the bubble point pressure, T is the fluid temperature, R_{sb} is solution gas-oil ratio and γ_g is the specific gravity of gas.

3.2.2 Compositional terms

GOR

The gas-oil ratio is the ratio between the volumetric gas flow and the volumetric oil flow at standard conditions. This shows the amount of gas that is associated with the oil flow. GOR can be expressed by:

$$\mathrm{GOR}\left[\frac{\mathrm{Sm}^3}{\mathrm{Sm}^3}\right] = \frac{Q_g}{Q_o} \tag{3.9}$$

GLR

The gas-liquid ratio is the ratio between the volumetric gas flow and the total volumetric liquid flow. It shows the amount of gas that is associated with the total liquid flow and can be expressed as:

$$\mathrm{GLR}\left[\frac{\mathrm{Sm}^3}{\mathrm{Sm}^3}\right] = \frac{Q_g}{Q_l} = \frac{Q_g}{Q_o + Q_w} \tag{3.10}$$

Water-cut

Water Cut (WC) is the ratio between the volumetric water flow and the volumetric liquid flow. WC can be expressed by:

$$\mathrm{WC}\left[\frac{\mathrm{Sm}^3}{\mathrm{Sm}^3}\right] = \frac{Q_w}{Q_l} = \frac{Q_w}{Q_o + Q_w} \tag{3.11}$$

4 Development of OLGA Rocx model

For this study, a simulation model was developed using OLGA-Rcox. The methodology adopted to build this dynamic reservoir-wellbore model is described along with a selection of different input parameters for the model.

4.1 Grid resolution and time step

The reservoir dimensions are listed in Table 4-1. Generally, the optimal length for inflow controllers is 12.4 m of the well. It was challenging to simulate with the normal AICDs, as it would require a significant amount of time as well as computational resources. So, an equivalent AICD was selected to represents the 8 normal AICDs. Hence, the length for an equivalent AICD is 99.2 (=12.4×8) m. Most of the cases are simulated with 10 equivalent AICDs, hence the length of the reservoir was taken as 992 m. Here, the flow area of an equivalent AICD is equal to the sum of flow areas of 8 normal AICDs.

Table 4-1: Dimension of the reservoir

Reservoir	**Span (m)**
Length (x)	992
Width (y)	80
Height (z)	20

The well is centrally located in the x-y plane at a height of 14 m from the bottom of the reservoir. Figure 4-1 shows the location of the well in the yz plane.

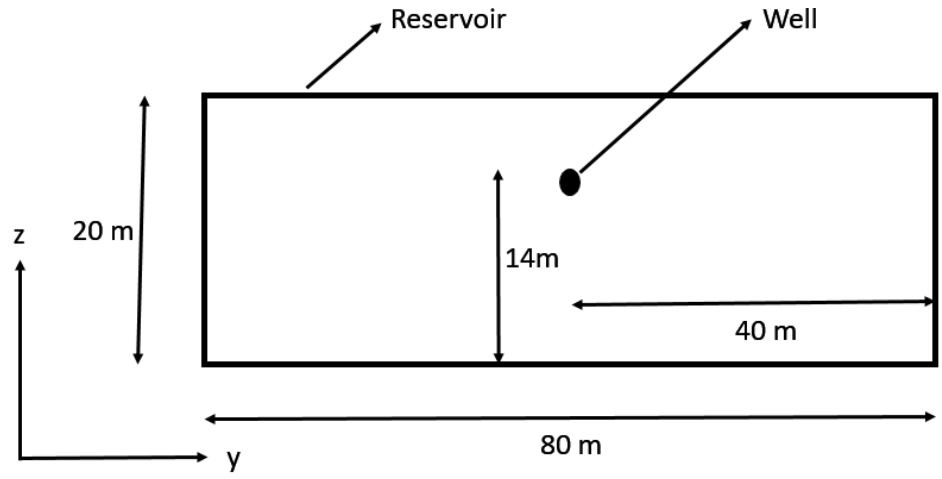

Figure 4-1: Location of the well in yz plane

The computational simulation should be accurate and time efficient. To achieve this, the optimal mesh and time step are required. Hence a finer mesh towards the well in y-direction was chosen. The simulation was done for 10 equivalents AICDs, hence the length was divided into 10 elements of constant size and the height was divided into 10 elements of constant size. The mesh size in a different direction is presented in Table 4-2.

Table 4-2: Number of elements and their sizes

Direction	Number of elements	Size of the element(s) (m)
x	10	99.2
y	29	3.5,3.5,3.5,3.5,3.5,3,3,3,2.5,2.5,2.5,2,2,1.5, 1,1.5,2,2,2.5,2.5,2.5,3,3,3,3.5,3.5,3.5,3.5,3.5
z	10	2

The three-dimensional view of the developed grid is shown in Figure 4-2.

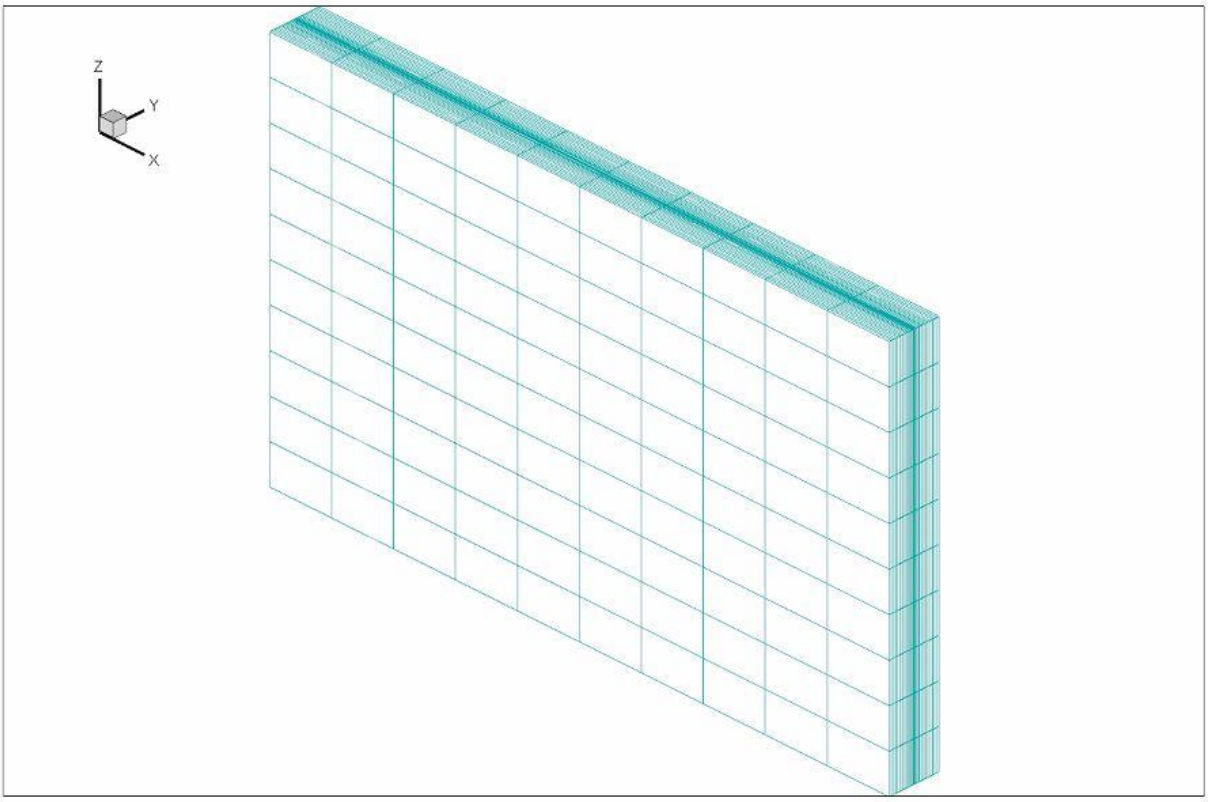

Figure 4-2: 3-D view of the grid

It can be assumed that the lowest time step gives the most accurate results, but considering the simulation time it takes, the minimum time step was set to 100 s. The maximum time step was set to 3600 s. The same minimum and maximum time step were used in all the simulations.

4.2 Development of the reservoir model

A reservoir model was developed in Rocx with the help of different reservoir properties. The boundary conditions and the initial conditions for simulation were specified in this model.

4.2.1 Grid

The dimension of the reservoir is given in Table 4-1. The mesh was created using the 3-D Cartesian coordinate system. The number of elements and their respective block length in each direction are tabulated in Table 4-2. The direction vector for gravity was set as 1 in the z-direction. This means that the first layer of the reservoir lies on the top and the subsequent layers lie below this.

4.2.2 Fluid Properties

In this section, the black oil model was selected over PVT table model. The basic properties of light and heavy oil used for the simulation are presented in Table 4-3. These values were considered at measured reservoir temperature of 100°C and pressure of 130 bar.

Table 4-3: Oil properties used for simulations

Parameters	Values (Light oil)	Values (Heavy oil)
Oil viscosity (cP)	3	150
Oil specific gravity	0.85	0.92
Gas specific gravity	0.64	0.64
GOR(Sm^3/Sm^3)	150	50

The LASATER model was chosen as the GOR model, as the API index lies in between (17.9° < API < 51.1°) [16]. Oil viscosity tuning was also enabled and the fraction type was selected as a mass fraction.

The black oil components, i.e., oil, water and gas components were defined according to Table 4-3.

This simulation was done with the bottom water drive. So, for simulation with water drive, two feed stream were defined for oil and water. These feed streams (light oil) are presented in Table 4-4.

Table 4-4: Feed streams

Stream	Fraction type	Fraction	Watercut
Oil	GOR	150	0.0001
Water	GLR	0.0001	0.99

4.2.3 Reservoir Properties

The porosity of the reservoir was taken as 0.3 and is constant throughout the reservoir. The permeability in each direction was defined by giving a value for each block in the reservoir in the respective direction. The simulated reservoir model based on the permeability profile were as follows:

- Fractured reservoir with a very high permeable zone (High permeable zone represents a fracture zone in the reservoir)
- Heterogeneous reservoir with one relatively high permeable zone and with one relatively low permeable zone
- Homogeneous reservoir

The horizontal permeability was taken as 10 times higher than the vertical permeability in each block of the reservoir. The vertical permeability profiles of these reservoirs are shown in Figure 4-3.

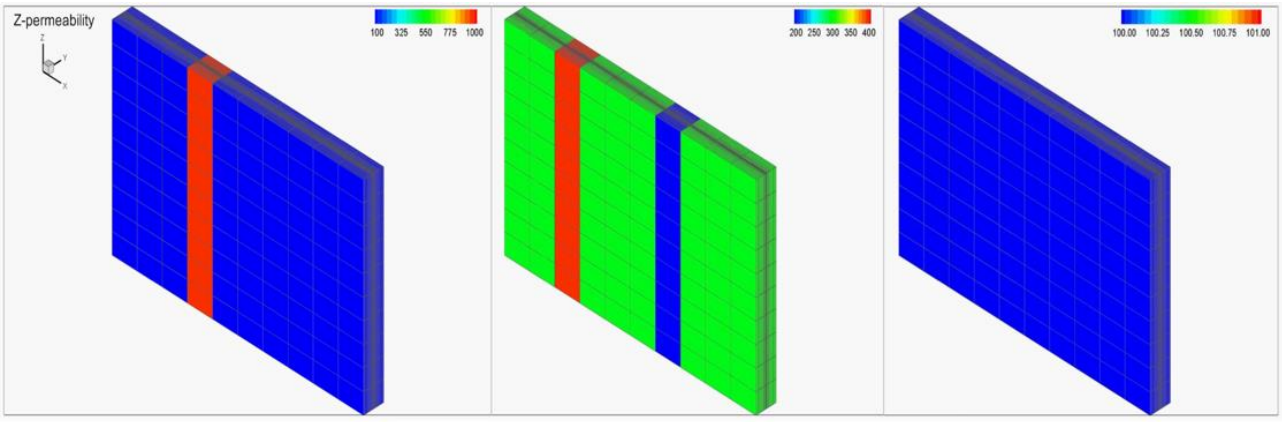

Figure 4-3: Vertical permeability profile

4.2.4 Relative permeability

The default values in the Rocx model were used for the relative permeability. The developed relative permeability curve is presented in Figure 4-4.

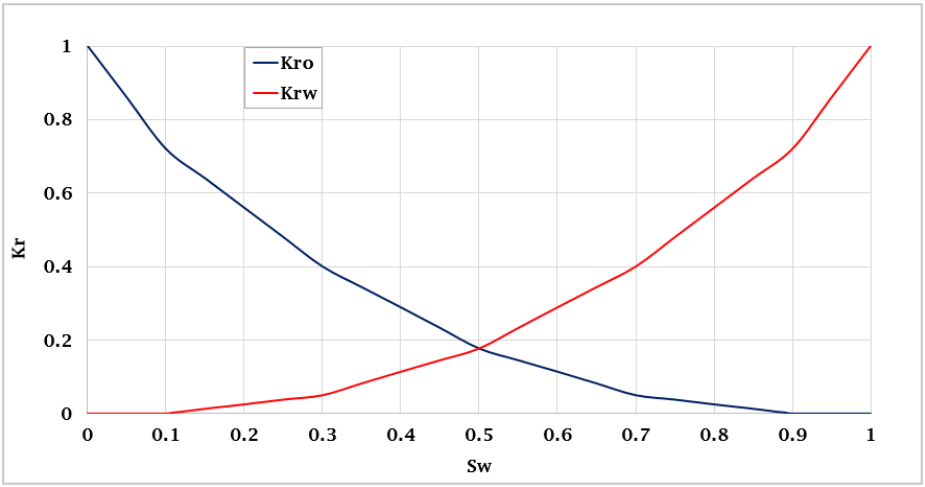

Figure 4-4: Relative permeability curves

4.2.5 Initial conditions

Initially, the black oil feed was defined as 100% oil and the reservoir were fully saturated with oil. The reservoir temperature is 100°C and the reservoir pressure is 130 bar.

4.2.6 Boundary conditions

4.2.6.1 Pressure (well)

The mesh was divided into 10 zones in the x direction, and due to this, the well was also divided into 10 zones. The position of the well, its radius, and the main flow direction for the well had to be specified for each zone. As shown in Figure 4-1, the well lies at the center of the y-axis, hence the grid block number is 15 along the y-direction. Similarly, the well lies 6 m below the top boundary, so the grid block number is 3 along the z-direction. The grid block number was set as 1 to 10 along the x-direction as the well lies along the x-direction. The main direction of flow in the well was set along the x-direction and the diameter of the well was taken as 0.1m. The well temperature and pressure were set to 100°C and 100 bar and the feed was defined as the oil feed.

4.2.6.2 Pressure (reservoir)

This simulation was based on the bottom water drive. This boundary condition was defined in this section, i.e., the position of water drive and its main flow direction. The water aquifer lies at the bottom throughout the reservoir and the main direction of flow of water drive was set in the z-direction. The water drive temperature and pressure were also set to 100°C and 100 bar and the feed was defined as water drive feed.

4.2.7 Simulation

The simulation was performed using a linear iterative solver named ‘Linsolver’. The minimum time step was set to 100s and the maximum time step to 3600s, with an initial time step of 0.01s.

4.3 Development of well and wellbore model

The well and the wellbore model was developed using different process equipment modules in the OLGA GUI. This chapter gives the information about the model.

4.3.1 Case definition

The basic parameters of the model and the simulation criteria were specified in this section. The compositional model was chosen as black oil with 1st order discretization scheme for solving mass equations. The simulation was conducted as dynamic three phase system. The maximum and minimum time steps were set to 3600s and 100s for simulation. Those cases were simulated for different periods of time. The simulation was based on isothermal conditions in the interface between the well and the reservoir.

4.3.2 Compositional

The three black oil components for oil, water and gas and the feeds for oil and water drive were specified in this section. These components and feeds were defined the same way as defined in Rocx.

4.3.3 Flow Component

In this section two pipes were used, one to represent the well (Flowpath) and another to represent the annulus (Pipeline) section of the flow system. The length was of 992m and diameter 0.1m. The surface roughness was set to 5^{-05} m and discretized into ten zones and each zone was divided into two sections. The concept of this model is shown in Figure 4-5.

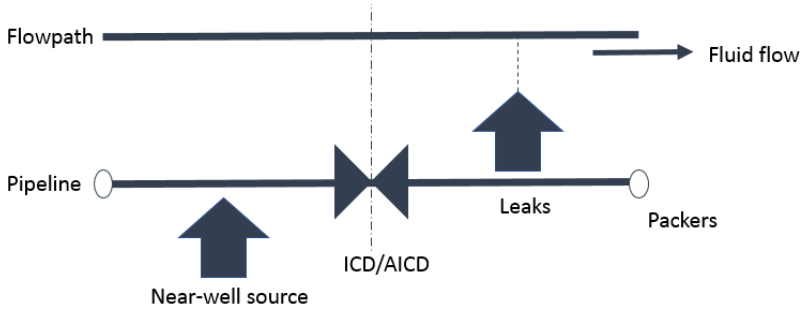

Figure 4-5: Representation of single zone of well

The inflow from the reservoir source (Near-well source) enters the pipeline from section 1. Then this fluid passes through the inflow controllers into section 2. Now, this fluid enters the Flowpath at section 2 from pipeline via leaks. The different zones of annulus were separated by means of a closed valve (opening = 0) which represents a packer. This packer ensures that there is no flow across each zone within the annulus section. Finally, the fluid gets collected from each zone in the well and moves towards the heel section of the wellbore. The OLGA modules that were used to develop this model are presented in Table 4-5.

Table 4-5: Components used in OLGA

Components	OLGA module	Description
Inflow source	Nearwell source	Coupled with reservoir model (Rocx file)
Leak	Leak	Diameter – 35 mm, CD[1] – 1 No mass transfer between the phase Connects to the Flowpath
ICD	Valve	Diameter – 20 mm, CD – 0.84 The diameter of the valve was used to decide the required pressure drop.
AICD	Valve/PID controller	Diameter – 20 mm, CD – 0.84 The valve opening was controlled by a PID controller
Packers	Valve	Diameter – 0.1 m, opening – 0 (fully closed)

The boundary condition of pipeline and the flow path were defined according to Table 4-6.

Table 4-6: Boundary conditions in OLGA

Components	Boundary	Boundary type
Pipeline	Inlet	Closed
	Outlet	Closed
Flowpath	Inlet	Closed
	Outlet	Pressure • Pressure – 120 bar (light oil) • Pressure – 110 bar (heavy oil) • Temperature- 100°C

[1] Coefficient of Discharge

4.3.4 AICD modeling

The AICD is an autonomous inflow control device, which opens or closes when the specific fluid passes through it. A valve module controlled by a PID controller module in OLGA was used to simulate as an AICD. The control variable for this PID controller was in situ water cut percentage (75%) which was transmitted to the PID controller by means of Transmitter module in OLGA. The PID controller used this control variable to close the valve once it reaches its setpoint. The parameters of the PID controller are defined in Table 4-7, to get a decent controlling action of the actuators (valves). These parameters were obtained by means of trial and error methods.

Table 4-7: PID controller parameters

Parameter	Value
Amplification	-0.01
Bias (Initial signal)	1
Integral constant [s]	50
Maximum signal (maximum opening)	1
Minimum signal (minimum opening)	0.01

4.4 Simulated cases

The three main type of reservoir mentioned in Figure 4-3 was simulated. The fractured reservoir was more focused due to the fact that early water breakthrough was expected. This environment was particularly favorable to see the capabilities of different inflow control technologies for controlling the early water breakthrough. The simulations were based on light and heavy oil, their specifications are presented in Table 4-8.

Table 4-8: Simulated cases based on types of oil

Cases / Properties	Heavy oil case	Light oil case
Oil viscosity (cP)	150	3
Gas-Oil ratio (GOR)	50	150
Oil-specific gravity	0.92	0.85

The cases based on the types of inflow control technologies are listed in Table 4-9. Results obtained from these different cases were compared with each other.

Table 4-9: Types of simulated inflow control technologies

Case 1 (ICD)	Wells with ICDs (Diameter – 20 mm, CD – 0.84)
Case 2 (AICD)	Wells with AICDs having relative opening of 1% when it is in closed position (Diameter – 20 mm, CD – 0.84)
Case 3 (ICD_{res})	ICD with relatively high flow restriction at the high permeable zone (Diameter – 0.2mm) and normal ICDs in the rest of the zones

The results from these simulations were studied for the different reservoir and further some other cases were designed and simulated based on the positive features of these simulated cases. These new cases involve a change in parameters like oil viscosity, the minimum opening of PID controller module to see the overall effects on the model performance.

The following data from the different simulations were considered for comparison of different cases:

- Accumulated oil, water, and total liquid (m^3) with time
- Volumetric flow rate of oil, water, and total liquid at standard conditions (Sm^3/d) with time
- Pressure profile across the pipeline
- Measurement signal of the PID controllers
- Relative opening of AICD

5 Simulation results

This chapter contains all the simulation results for the different cases that have been studied during this thesis work. The functionality of the AICD and ICD was studied and analyzed for different cases. The goal of this simulation study is to optimize the oil production and limit the water production with the help of inflow control devices for different types of reservoirs. The light oil case for the fractured reservoir is described in greater details than the other cases.

5.1 Analysis of light oil case

The simulations were performed with light oil for the different cases presented in Figure 4-3.

5.1.1 Fractured reservoir

Figure 5-1 shows the flow rate and accumulated liquid with ICD for the fractured reservoir. The first water breakthrough occurs after 9 days of production.

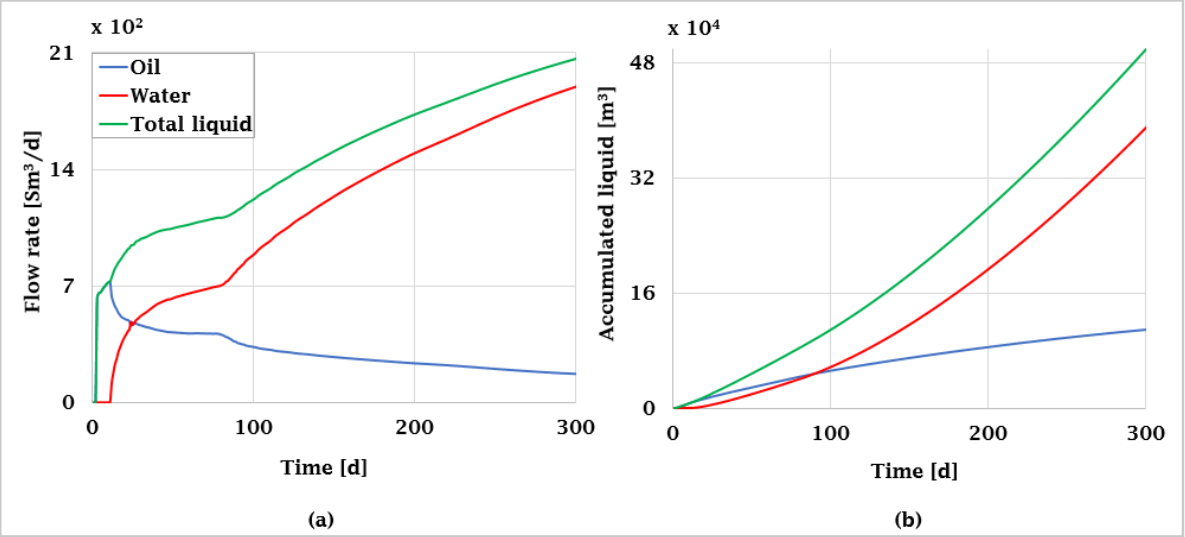

Figure 5-1 (a): Flow rates, (b): Accumulated liquid for ICD case (light oil)

As soon as water breakthrough occurred, the oil volume flow decreased and water volume flow increased significantly. There is a gradual increment in water flow rates after 76 days of operation which indicates that the second water breakthrough has occurred. As a result, the accumulated volume of water is more than twice the accumulated oil volume after 300 days. This shows that the system is producing oil with relatively high water cut, which is not suitable for an economical production.

Figure 5-2 shows the water cut profile along the wellbore after 300 days of production. It shows that the system is producing oil with more than 80% water. The water cut profile towards the heel segment is relatively higher because of high water production from the high permeable zone.

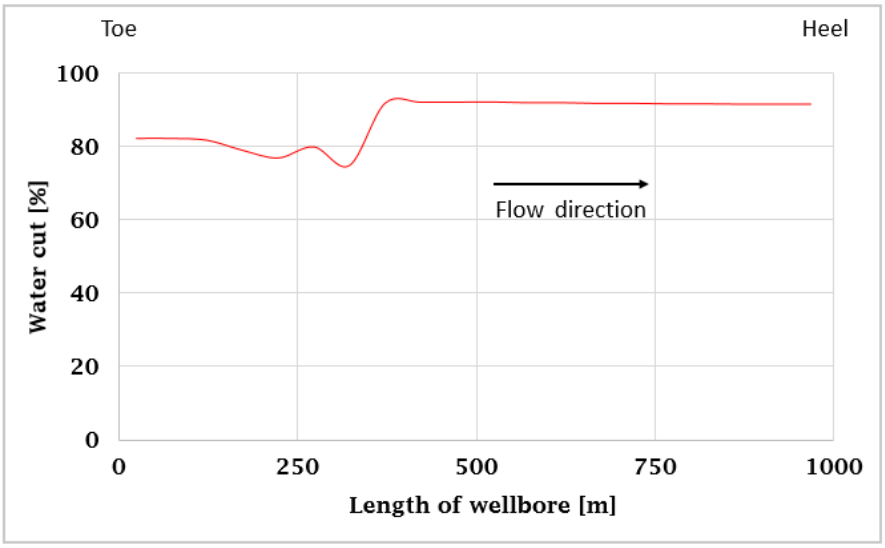

Figure 5-2: Water cut profile along the length of well after 300 days.

Further, from Figure 5-1, it can be seen that the water volume flow rate exceeds the oil volume flow rate after 24 days of production. During these early days, the production is dominated by the production from the fractured zone. This behavior can be visualized by the oil saturation profile in the fractured zone together with the relative permeability of oil and water.

Figure 5-3 shows the oil saturation profile of the high permeability zone of the reservoir after 24 days of oil production. The water saturation[2] is almost 0.5 around the well and continuously increases further. The red and blue color represents 100% oil and 100% water respectively.

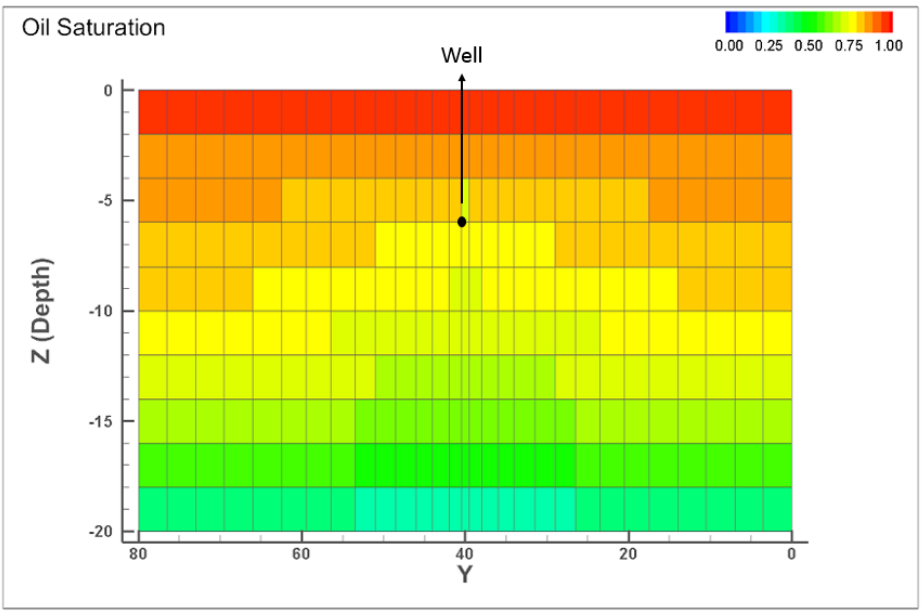

Figure 5-3: Oil saturation profile for fractured zone

[2] Water saturation = 1- Oil saturation

Figure 4-4 shows that the relative permeability of water is higher than that of oil at water saturation higher than 0.5. Hence, the water flow rate dominates the oil flow rate after 24 days.

Since the simulated case has a high permeability zone and 9 low permeability zones, water breakthrough was observed at two different times. The first water breakthrough was observed from the high permeability zone and the second breakthrough was observed from all the other zones. This can be seen from the oil saturation profile of the reservoir. The oil saturation profile of the reservoir after 9 days of production is shown in Figure 5-4. The first water breakthrough occurred only from the fourth zone, whereas the water inflow from the other zones is just starting to develop from the bottom.

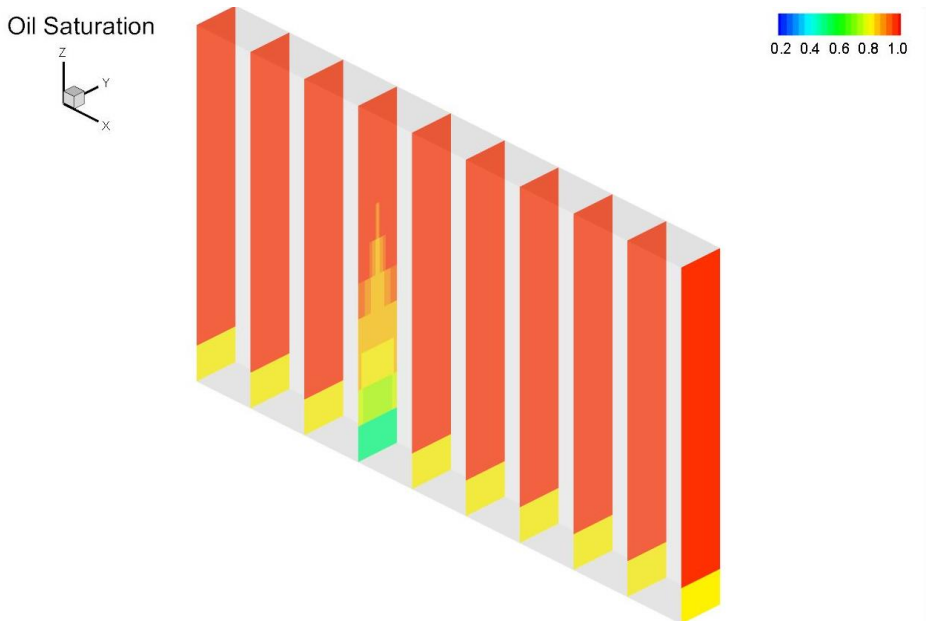

Figure 5-4: Oil saturation profile after 9 days (ICD)

The oil saturation profile for the zones 1(toe), 6 and 10 (heel) are presented in Figure 5-5. They are plotted after 76 days of operation. There is a complete conical water saturation profile in Zone 10.

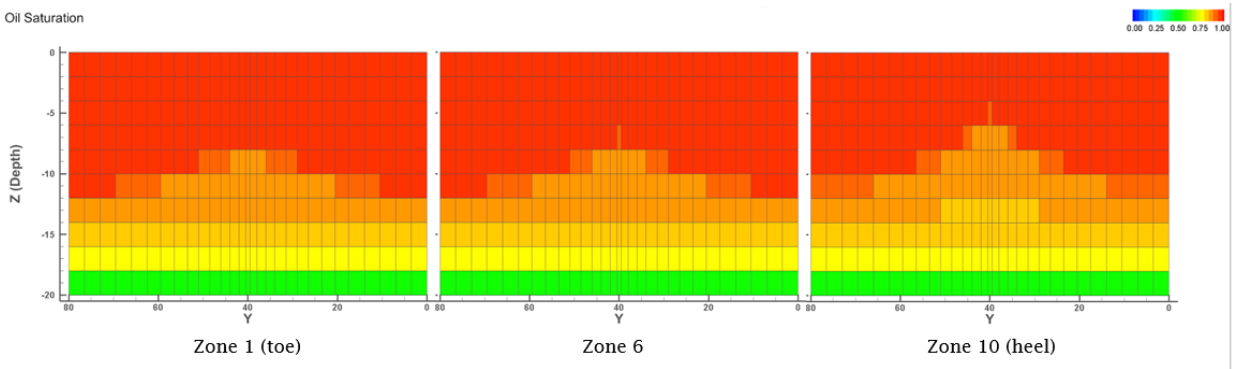

Figure 5-5: Oil saturation profile after 76 days

In real practice, conical water saturation profile is obtained after a water breakthrough. This can justify that these simulations approach the real phenomenon of this process. The water cones in the toe and the Zone 6 are still developing compared to the heel section. This shows that there is some heel to toe effects in the well due to frictional pressure drop.

So, in the fractured reservoir, the early water breakthrough takes place from zones with higher permeability. After the water breakthrough, the water flow rates exceed the oil flow rates, regardless of the oil production from the rest of the zones. Therefore, it is essential to install more efficient inflow control devices for producing oil at low water cut. Hence, different inflow control technologies were studied during this work. The restrictive ICD (non-uniform ICD) and AICD were studied. The non-uniform ICD model has relatively high flow restriction and is installed in the high permeable zone (Diameter – 0.2mm: - 1% of normal diameter). Normal ICDs (Diameter – 20mm) are installed in the rest of the zones.

The results for the fractured reservoir are presented below. The fourth zone from the toe end of the wellbore has significantly higher permeability compared to the other zones in this reservoir. The accumulated oil and water are presented in Figure 5-6.

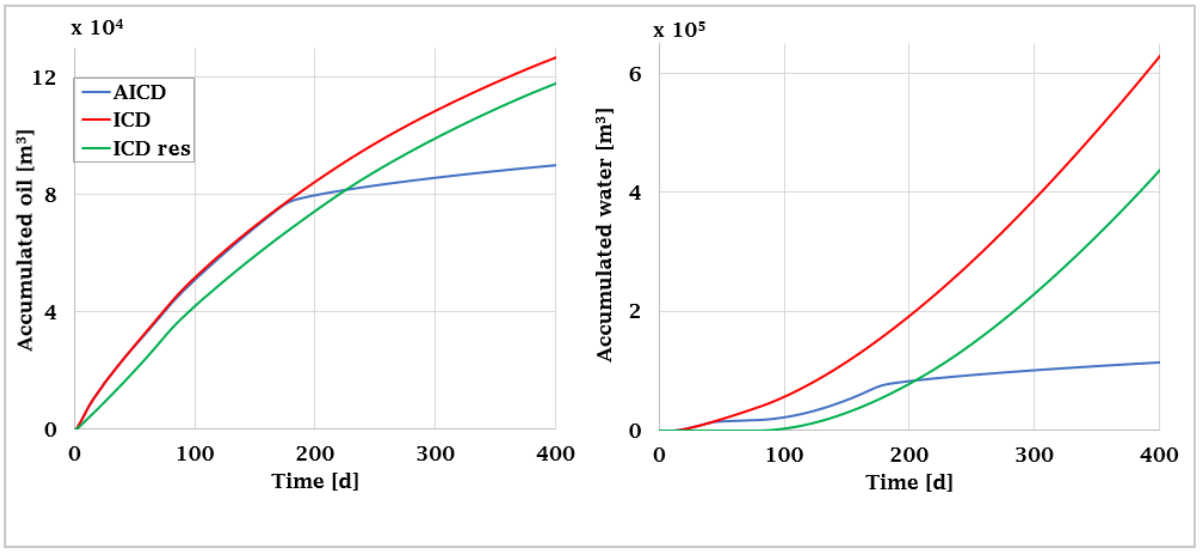

Figure 5-6: Accumulated liquid for fractured reservoir (light oil)

Accumulated oil and water volume are the most important parameters for comparing the performances of different inflow controllers. The case with AICD has the highest potential to reduce the water accumulation among the considered inflow control technologies. The ICD case with restriction gives less accumulation of water compared to normal ICDs. The accumulated oil and water volume with different inflow control technologies are presented in Table 5-1. These results were obtained after 400 days of production.

Table 5-1: Accumulated liquid comparison

Case	Accumulated oil [m^3]	Accumulated water [m^3]
ICD	127145	634733
AICD	89943	113654
ICD res	118123	441054

These data show that the non-uniform ICD case can be a good option to reduce the accumulated water. The restriction imposed on high permeability reduces water accumulation by 30% compared to normal ICD. However, the autonomous device gives remarkably higher potential of reducing water influx. The AICD case produces 82% less water compared to the normal ICD case. As both AICD and non-uniform ICD have reasonable potential to control water inflow causing a slight change in oil production, they have to be studied further depending on the types of applications.

The liquid flow rates with different inflow control technologies for the fractured reservoir are presented in Figure 5-7. There are significant changes in the oil and water flow rates throughout the production time. This illustrates the features of the different inflow controllers.

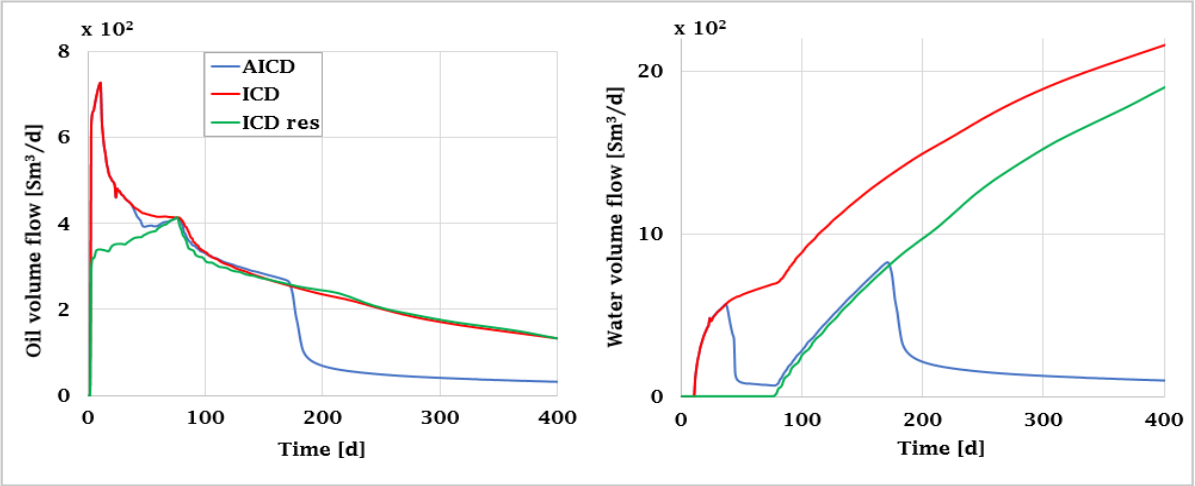

Figure 5-7: Liquid flow rates for fractured reservoir (light oil)

According to Figure 5-7, initial water breakthrough occurs on day 9 of production for the cases with AICD and normal ICD. Once the water is produced, the oil volume flow rate decreased significantly.

By installing a higher restrictive ICD with higher pressure drop, in the high permeable zone, the first water breakthrough has been delayed to 76 days of operation which is the same as the second water breakthrough for the two other cases. The oil production has also been reduced due to the introduction non-uniform ICDs. Table 5-2 shows the accumulated oil after the first and second water breakthrough.

Table 5-2: Oil production at breakthroughs

Case	1st breakthrough	Accumulated oil after 1st breakthrough [m3]	2nd breakthrough	Accumulated oil after 2nd breakthrough [m3]
ICD	9 days	6889.74	76 days	42116.82
ICD res	76 days	32979.17	-	-
AICD	9 days	6889.74	76 days	41005.28

The accumulated oil with AICD is slightly less than that of normal ICD at the time of the second breakthrough because of the closure of autonomous device from the fractured zone. It can be seen that the non-uniform ICD model has the capability to delay water breakthrough by 67 days in this reservoir. This is the most positive features of this model, while its inability to restrict water influx after breakthrough is the drawback. It is challenging to find the precise location of the high permeable zone, and therefore there would be a high risk installing restrictive ICD.

Figure 5-6 shows that the restrictive ICD model has been able to delay the water breakthrough significantly. However, the accumulated water goes on increasing after breakthrough occured. This indicates that the autonomous model has large benefits compared to other models.

Figure 5-8 shows the closing patterns of all the valves for AICD where Valve 4 closes after 45 days of operation while rest are completely shut off after 180 days of operation. As soon as the autonomous valve in the high permeability zone (Valve 4) starts closing, the flow profile of the AICD and normal ICD deviates from each other. The volume flow of both oil and water with AICD is significantly reduced after the closure of all the autonomous valves.

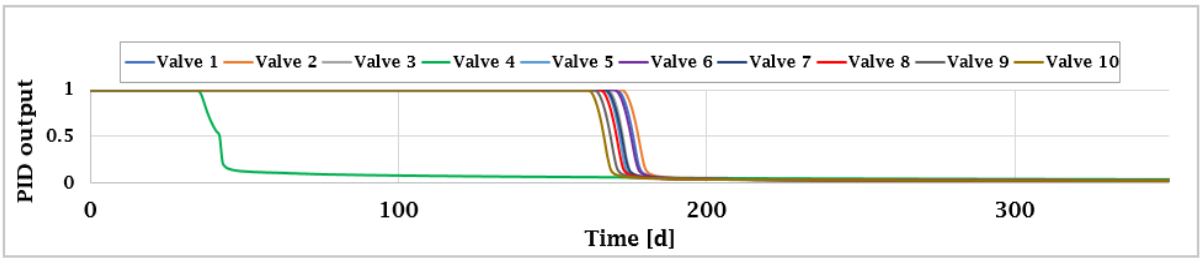

Figure 5-8: Closing patterns of autonomous valves

The graphs show that it takes more than 20 days for a valve to reach a fully closed position from the fully open position. If the autonomous devices take relatively long time to get closed, the water influx will be increased. Also, the relative opening when the valves are in closed position would also affect the oil and water production rates. The behavior of changing the minimum opening and changing the pressure drop over AICD is presented in Chapter 5.4. The design parameters have to be considered based on the types of application along with the financial budgets of the projects.

Further, the effect of changing parameters like oil viscosity, mesh size for the fractured reservoir is presented in Chapter 5.3.

5.1.2 Homogeneous reservoir

The liquid flow rates for the homogeneous reservoir are presented in Figure 5-9.

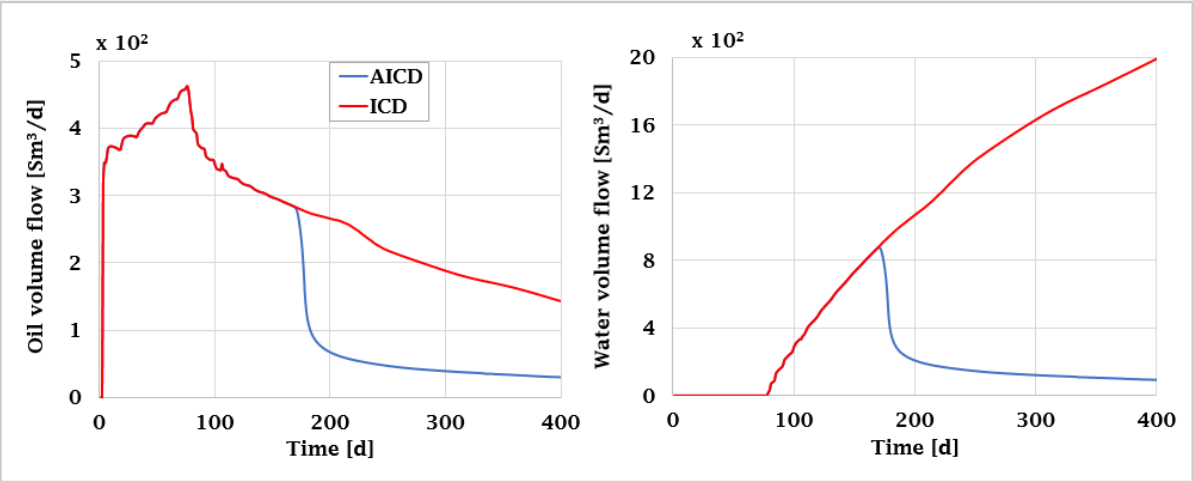

Figure 5-9: Liquid flow rates for homogeneous reservoir (light oil)

The oil volume flow increases continuously and reaches 456 Sm^3/d just before the water breakthrough. After the water breakthrough at 75 days, the oil volume flow decreases and the water volume flow increases. There has been continuous decrease of oil flow rate and increase of water flow rate after breakthrough for the ICD case. The flow rates for the AICD case are heavily reduced after closing of the valves. Hence the oil saturation profile for all the zones is almost the same when the toe-heel effect is insignificant. Therefore, water breakthrough occurs at about the same time in all the zones. As a consequence, all the AICDs close within a short time interval.

Figure 5-10 show the oil saturation for different zones inside the homogeneous reservoir. Water saturation from the bottom is continuously growing equally throughout the reservoir. Hence the use of the autonomous device is not so significant when the frictional pressure drop along the wellbore is insignificant. The frictional pressure drop was observed to be around 0.2 bar just before the water breakthrough.

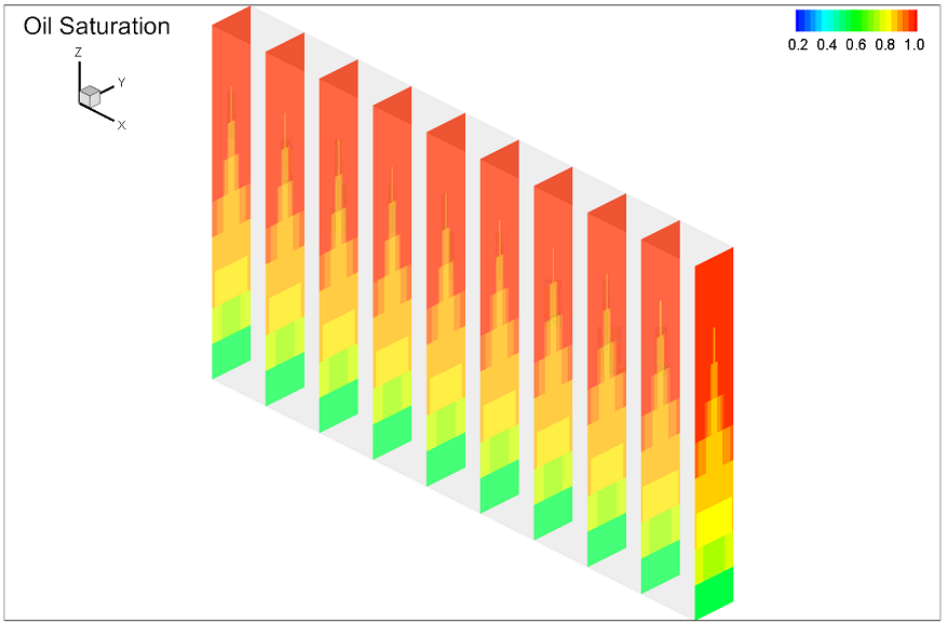

Figure 5-10: Oil saturation profile after 75 days for homogeneous reservoir

Further, the study of accumulated liquid can show the functionality of ICD and AICD. Figure 5-11 shows the accumulated liquids for the homogeneous reservoir.

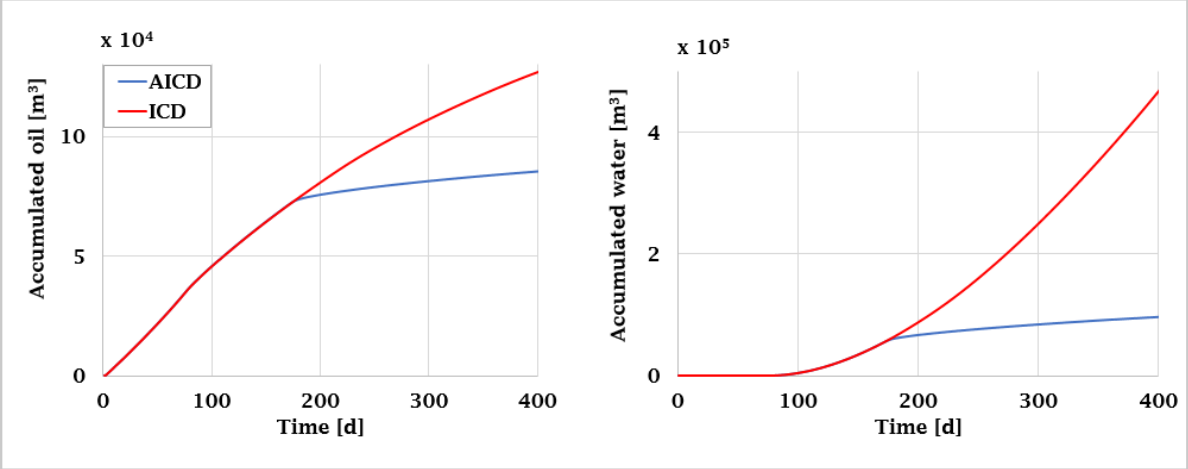

Figure 5-11: Accumulated liquid for homogeneous reservoir (light oil)

There has been a continuous increment of accumulated oil with ICD while it drops for the case with AICD after closing the valves. Once the water breakthrough has started, accumulated water is also increasing continuously for ICD. The autonomous inflow controllers are able to reduce the water significantly. Although there has been a reduction in accumulated oil, the accumulated water reduces by 80 % with the use of autonomous devices.

5.1.3 Heterogeneous reservoir

The results for the heterogeneous reservoir are presented below. This is an intermediate reservoir between the homogeneous and fractured reservoir. It has one zone with relatively

high permeability and one zone with relatively low permeability compared to the rest of the zones. The liquid flow rates at standard conditions are presented in Figure 5-12.

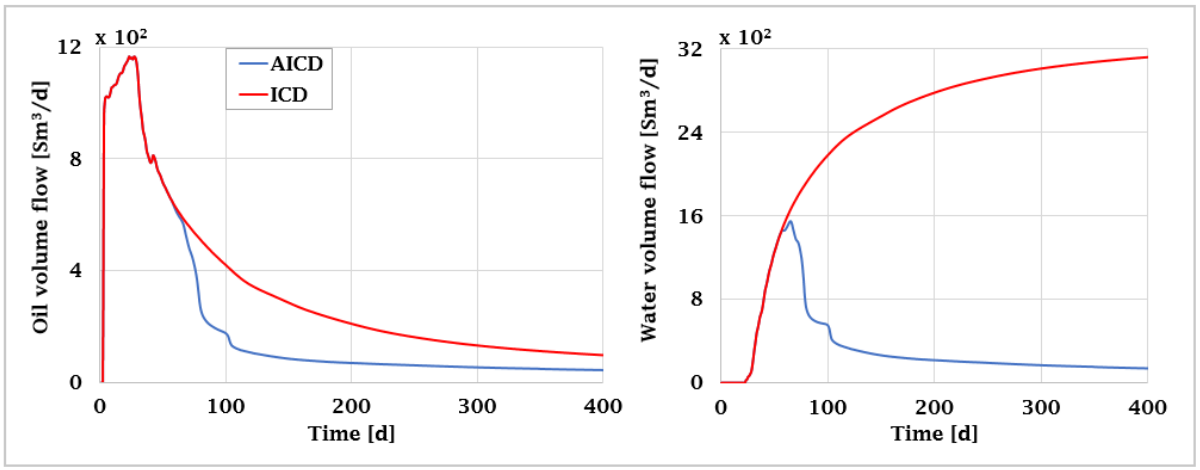

Figure 5-12: Liquid flow rates for slightly heterogeneous case (light oil)

The plots show that the oil volume flow reaches a maximum value of 1156 Sm^3/d and reduces considerably once the water breakthrough has occurred. The water breakthrough was seen on day 25 from the start of the operation. The closing of the first valve is from high permeability zone. This can be visualized from the oil saturation profile of the reservoir. Figure 5-13 shows the oil saturation profile after 25 days for this heterogeneous reservoir.

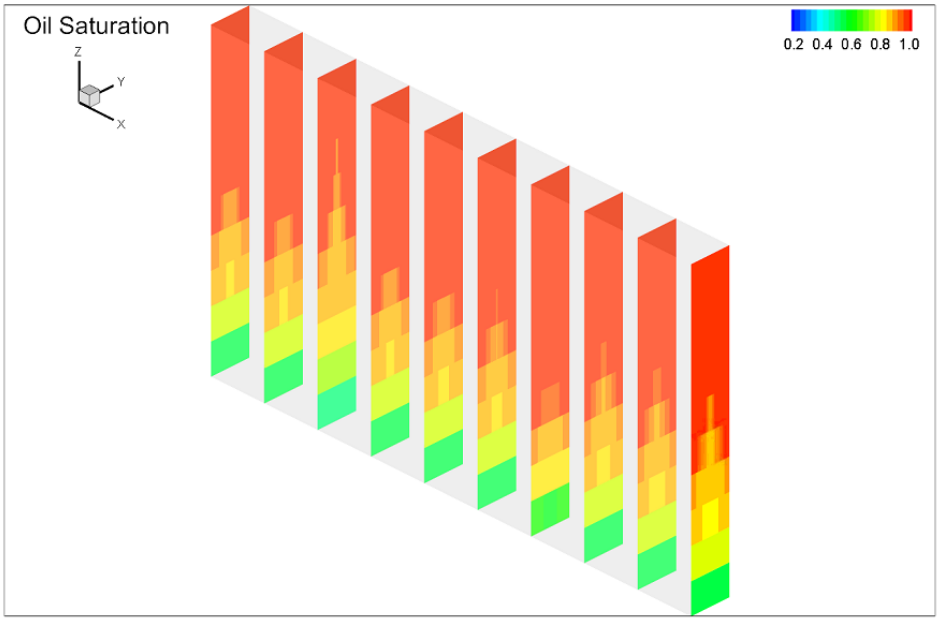

Figure 5-13: Oil saturation profile after 25 days of oil production

Water from the Zone 3 reaches the wellbore early compared to other zones. The water profile in Zone 7 is still developing beyond the others because of its low permeability. The valve from this zone is the last one to get choked.

There is a reduction of liquid flow rates after the autonomous devices have been shut off. The water volume flow increases continuously and reaches around 3200 Sm^3/d with the use of ICD. This, in turn, gives high accumulation of water presented in Figure 5-14.

Figure 5-14 shows the accumulation of oil and water for this heterogeneous reservoir. The accumulation of oil gets reduced with the use of autonomous devices compared to that of ICDs. However, the accumulation of water reduces significantly by around 88% after 400 days of operation.

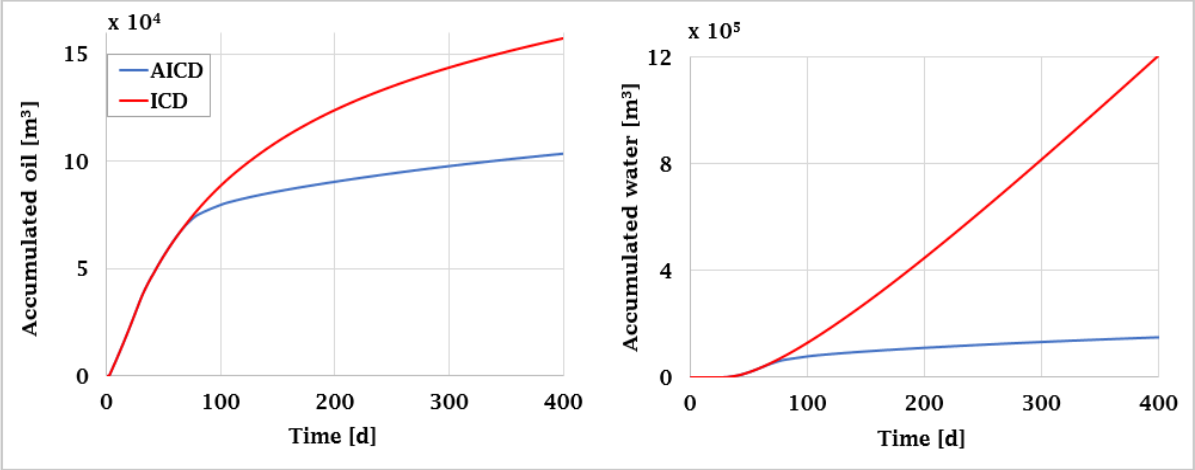

Figure 5-14: Accumulated liquid for slightly heterogeneous case (light oil)

From the above-obtained results for the three different types of the reservoir, AICD can be effectively used depending on the types of application. The water breakthrough for the homogeneous reservoir was seen after a long time period. Table 5-3 shows the comparison of AICD and ICD performances after 400 days of operation for these three reservoirs. The change of oil and water accumulation with the use of AICD and restricted ICD is presented with respect to normal ICD.

Table 5-3: Summary of results (light oil)[3]

☺	**Fractured reservoir**		**Heterogeneous reservoir**		**Homogeneous reservoir**	
	Accumulated oil [m^3]	Accumulated water [m^3]	Accumulated oil [m^3]	Accumulated water [m^3]	Accumulated oil [m^3]	Accumulated water [m^3]
ICD	127145	634733	157313	1217842	127406	472463
ICD res	118123 (-7.09%)	441054 (-30.5%)	-	-	-	-
AICD	89943 (-29.26%)	113654 (-82.09%)	103288 (-34.34%)	151559 (-87.55%)	85376 (-32.98%)	96201 (-79.64%)

[3] Percentage in bracket represents the change with respect to ICD

The data show an almost similar performance of AICD for the different types of reservoirs, but the main ability of AICD is to allow the normal oil production from the other zones by choking the flow from the high permeability zones. AICD has the highest reduction of water accumulation of around 88 % for the heterogeneous reservoir. Hence, this autonomous device is more suitable for the heterogeneous reservoir and fractured reservoir where it reduces the water accumulation significantly.

5.2 Analysis of heavy oil case

This chapter includes the results with heavy oil for different types of reservoir presented in Figure 4-3.

5.2.1 Fractured reservoir

Oil and water production potential of the fractured reservoir can be studied with the accumulated oil and water volumes. The accumulated oil and water volumes with respect to time are presented in Figure 5-15.

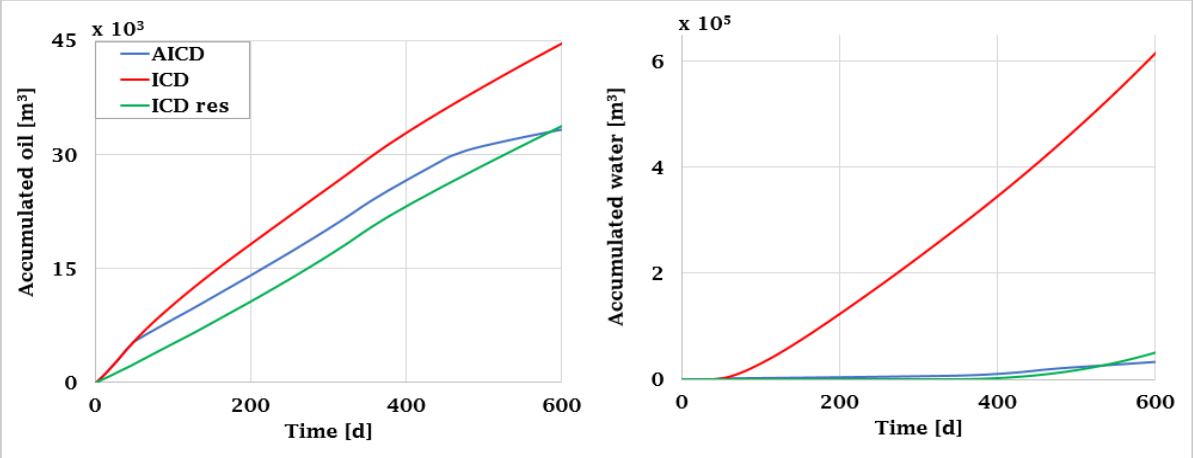

Figure 5-15: Accumulated liquid for fractured reservoir with heavy oil

The graphs show that early water breakthrough occurs on the 35 days of production. The potential of water production increases continuously after the water breakthrough. As a result, the accumulated water for the normal ICD case is around 14 times higher the accumulated oil after 600 days. This ratio for the non-uniform ICD case reduces to 1.5 and for the case with AICD to 0.97. This shows that there is a significant reduction of water accumulation with the use of AICD and non-uniform ICD.

Figure 5-16 shows the oil and water volume flow rates at standard conditions for the fractured reservoir.

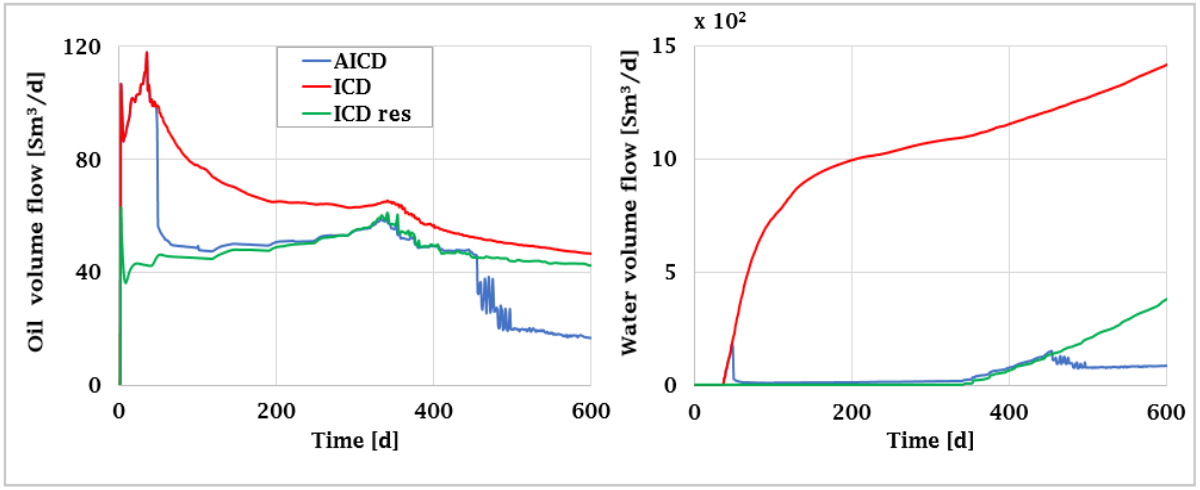

Figure 5-16: Liquid flow rates for fractured reservoir (heavy oil)

The oil volume flow rate reduced significantly after the initial water breakthrough with the use of ICD and AICD. The water breakthrough for a case with non-uniform ICD is delayed to 341 days of operation. This is the reason for low accumulation of water after 600 days with the use of non-uniform ICD. The closing of the AICD from the fracture zone after 50 days reduces both oil and water flow rates significantly. Further reduction of liquid flow rate was observed after the closing of AICD in low permeable zones. The water volume flow with the use of ICD is continuously increasing and reaches 1416 Sm^3/d after 600 days.

5.2.2 Homogeneous reservoir

The liquid flow rates at standard conditions for the homogeneous reservoir is presented in Figure 5-17.

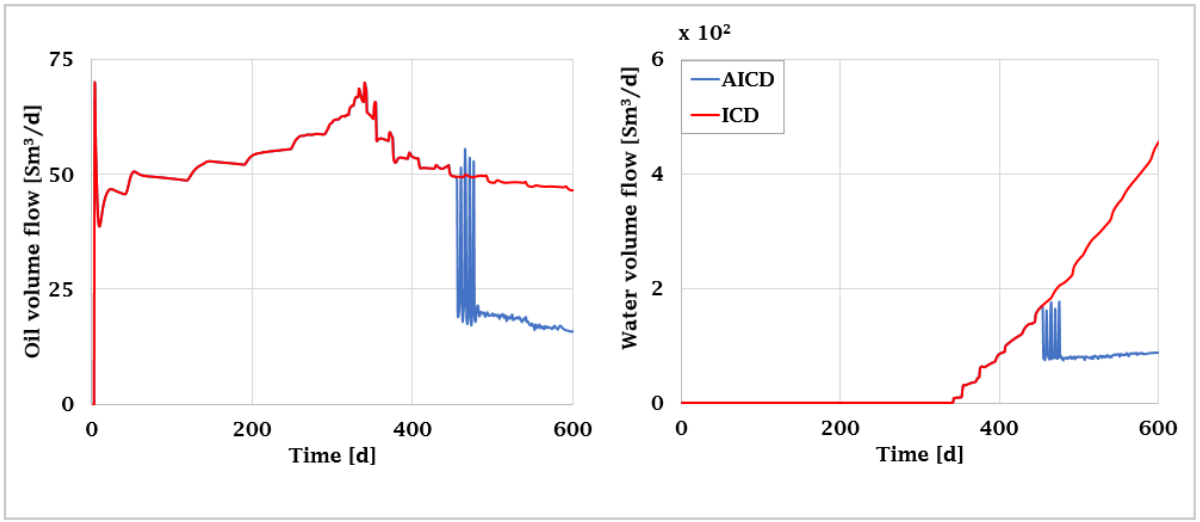

Figure 5-17: Liquid flow rates for homogeneous reservoir (heavy oil)

The plots show that the water breakthrough occurred after 340 days of production. When the reservoir does not have any high permeable zones, then the oil can be produced without water breakthrough for a longer period. This is the main characteristics of the homogeneous reservoir.

The oil production rate reduces and the water production rate increase continuously after the water breakthrough. The installations of AICD gives around 60% less water accumulation after 600 days compared to ICD, as shown in Figure 5-18.

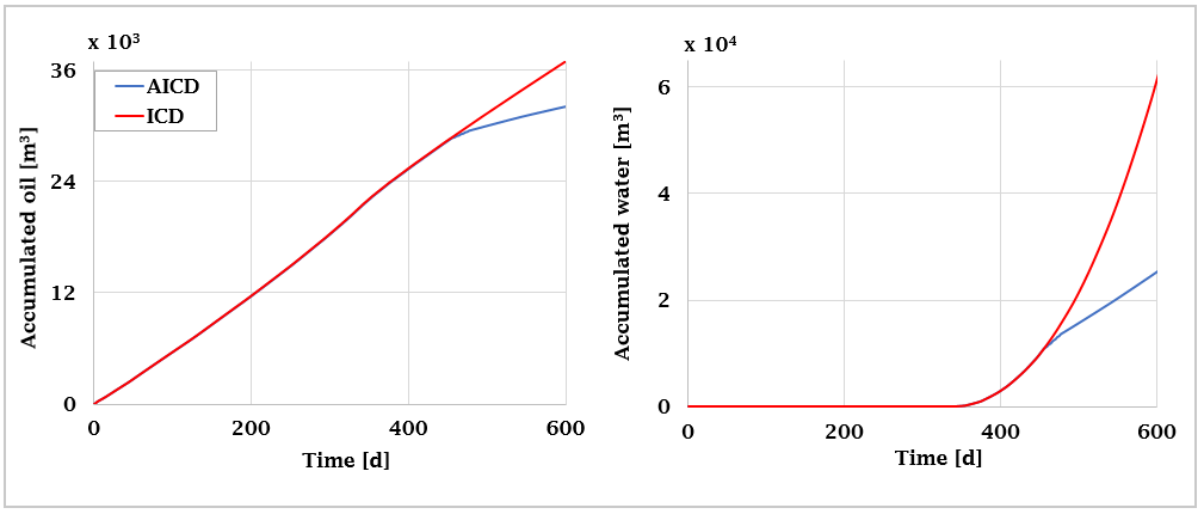

Figure 5-18: Accumulated liquid for homogeneous reservoir (heavy oil)

The graphs show the accumulated oil and water for a homogenous reservoir with respect to time. As expected, AICD has reduced the amount of accumulated water by 60%. Also, there has been about 13% reduction in oil accumulation. Figure 5-18 shows that the flow profiles with ICD and AICD cases deviates after the closing of autonomous devices.

5.2.3 Heterogeneous reservoir

The results for the heterogeneous reservoir is presented in this chapter. The accumulated liquid with respect to time is presented in Figure 5-19. The accumulation rate of oil with ICD increases continuously with time. The accumulation rate with AICD reduces after the closure of AICDs around 150 days. As a result, the difference in accumulated oil is significant after 400 days.

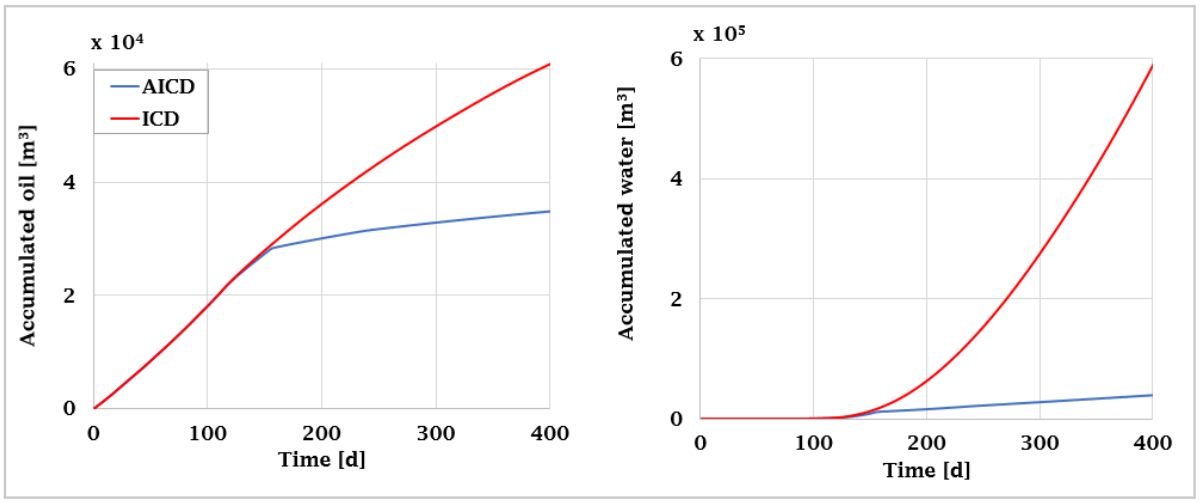

Figure 5-19: Accumulated liquid for slightly heterogeneous reservoir (heavy oil)

Water breakthrough occurred after 85 days, causing the accumulated water rising sharply with the ICD case. The accumulated water with AICD is considerably low compared to the ICD case. There is 93% reduction of accumulated water with the use of AICD compared to that of ICD after 400 days.

Further, the oil and water volume flow rates at standard conditions for the heterogeneous reservoir are presented in Figure 5-20.

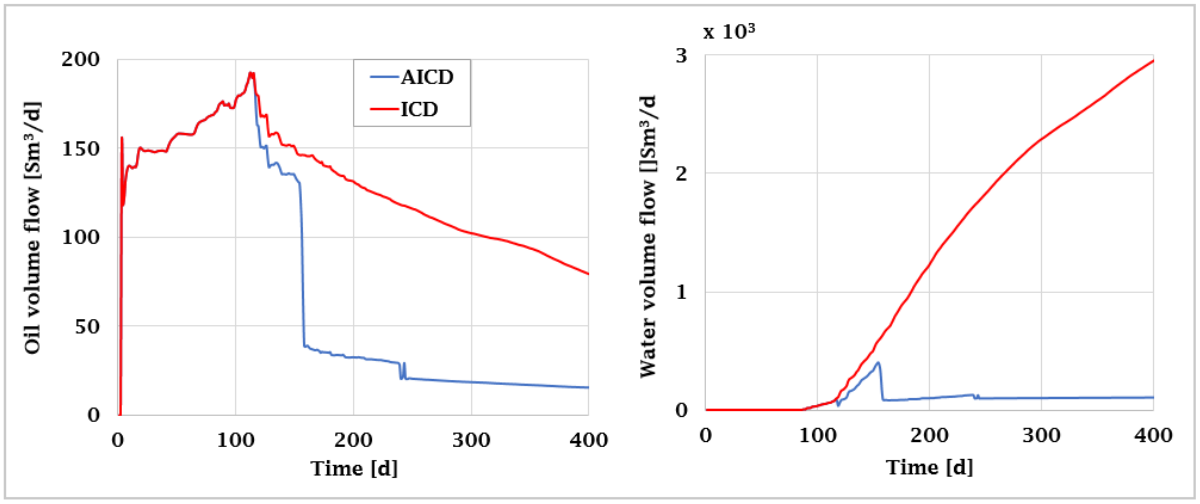

Figure 5-20: Oil and water flow rates for slightly heterogeneous reservoir (heavy oil)

Initially, there is a gradual increment of oil volume flow rate up to 113 days of production and reduces considerably once the reservoir has higher potential to produce water than oil. After the water breakthrough, the water flow rate increases significantly unless AICD is installed. Although, there is decreases in oil volume flow after closing of AICD, the water volume flow rate reduces significantly.

Table 5-4 shows the comparison of AICD and ICD performances for these three reservoirs. The change of oil and water accumulation with the use of AICD and restricted ICD is presented with respect to normal ICD.

Table 5-4: Summary of results (heavy oil)[4]

☺	**Fractured reservoir**		**Heterogeneous reservoir**		**Homogeneous reservoir**	
	Accumulated oil [m^3]	Accumulated water [m^3]	Accumulated oil [m^3]	Accumulated water [m^3]	Accumulated oil [m^3]	Accumulated water [m^3]
ICD	44649	618301	61141	597535	36997	62555
ICD res	33890 (-24.09%)	52503 (-91.5%)	-	-	-	-
AICD	33273 (-25.48%)	32370 (-94.76%)	34884 (-42.94%)	39826 (-93.33%)	32122 (-13.22%)	25427 (-59.35%)

Similar to light oil, the data show AICD is able to reduce a significant amount of accumulated water in the fractured and heterogeneous reservoir. AICD case is able to reduce oil accumulation by around 95% in fractured reservoir compared to the ICD case. The total flow was choked between the short interval of time for the homogeneous reservoir due to low frictional pressure drop in the wellbore.

5.3 Effects of different model parameters

5.3.1 Oil viscosity

This simulation was performed to see the effect of change of oil viscosity in the model. Light oils with oil viscosity of 3 cP, 1.5cP, and 0.8 cP were studied. The simulations were done with AICD for light oil in the fractured reservoir. The oil and water flow rates at standard condition are presented in Figure 5-21.

[4] Fractured and homogeneous – after 600 days & heterogeneous – after 400 days

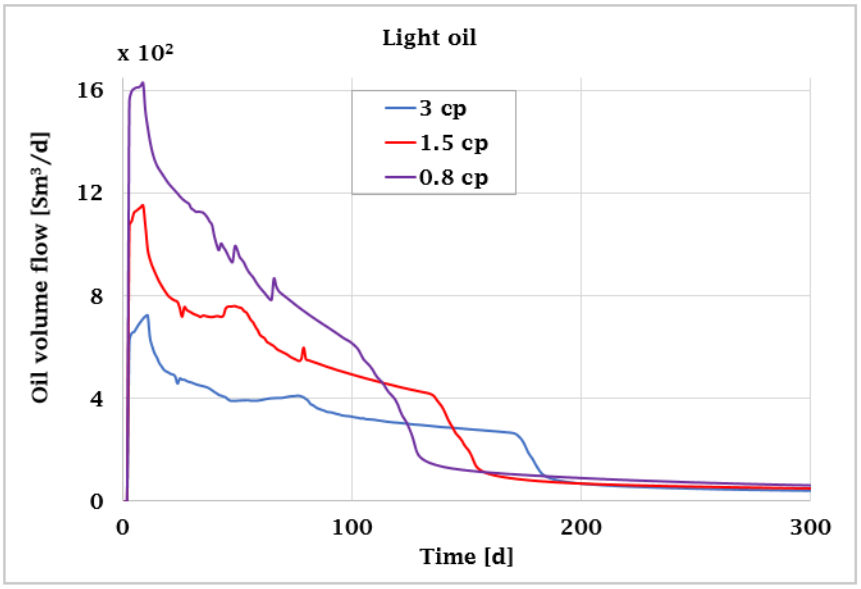

Figure 5-21: Liquid flow rates with different oil viscosity

The graphs show that the oil volume flow increases with the decrease of oil viscosity. The water breakthrough was observed earlier for the lesser light oil. The oil volume flow for the less light oil decreases more compared to others after water breakthrough.

The mobility ratio of oil with respect to water is given by Equation 5.1.

$$M = \frac{k_{rw}}{\mu_w} \cdot \frac{\mu_o}{k_{ro}} \tag{5.1}$$

This shows that, for a constant relative permeability of oil, water, and constant viscosity of water inside a reservoir, the mobility ratio is directly proportional to oil viscosity. As the oil viscosity decreases, the mobility ratio will decrease. And the expression for the definition of mobility ratio is given by the Equation 5.2.

$$M = \frac{\text{Mobility of water}}{\text{mobility of oil}} \tag{5.2}$$

Hence, the mobility of oil increases with the reduction of the mobility ratio. This is illustrated in Figure 5-21. The oil volume flow after the closing of autonomous valves is almost the same for all the cases as they all have the same minimum opening when the valve is in closed positions.

5.3.2 Mesh size

This study was done to see the effects of change of mesh size of the simulated reservoir. It can be argued that the finer grid gives more accurate results than the coarse grid. The grid along the y-direction was already finer close to the wellbore. It is interesting to see the results with more finer grids towards the x-direction also. Therefore, the mesh size in the x-direction were doubled in this study. This simulation was done with AICD for light oil in the fractured reservoir.

Figure 5-22 shows the liquid flow rates at standard conditions with two different mesh sizes along the flow direction.

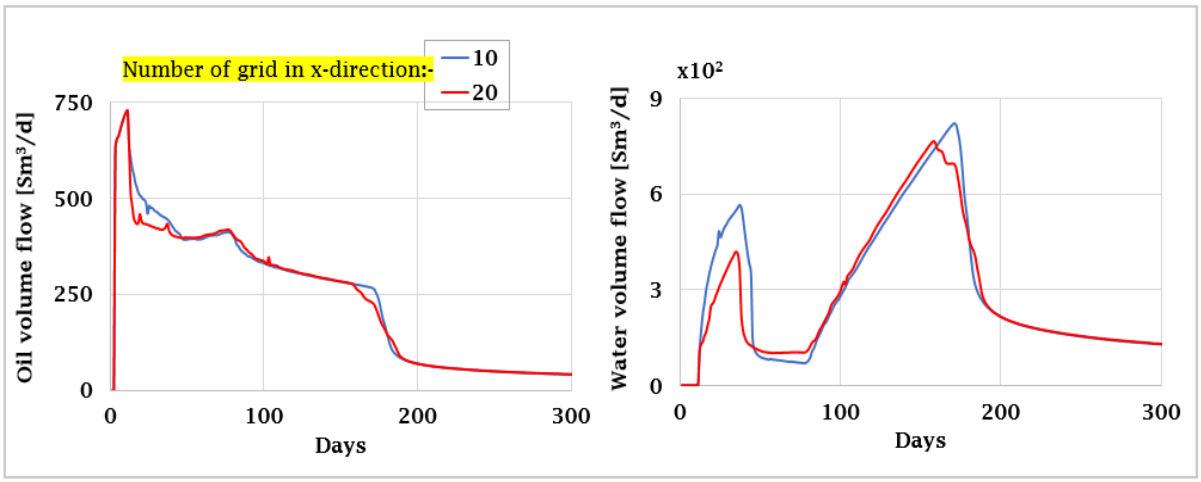

Figure 5-22: Oil and water flow rates for different mesh sizes

The flow rates with the increased grid deviate slightly from that of the normal grid. The oil volume flow is slightly different particularly during the closure of autonomous devices. The flow rates with 20 grid show closer overview of actual flow rates during this period. The water volume flow rate before the closure of valves also slightly differs from each other. But the flow rates after the closure of AICD is the same for both cases. It can be argued that the overall flow rate is little sensitive to the mesh sizes which is the good features of this model.

5.4 Effects of design parameters of AICD

The pressure drop across the valve and the allowable flow area at closed positions are the design parameters of AICD. Their parameters can be calibrated depending upon the types of application. The simulation results in Chapter 5.1.1, showed that if an ICD with the high pressure drop is installed in the high permeable zone, the first water breakthrough can be delayed. After the closing of AICD, the oil volume flow rate decreases significantly. However, if an AICD with the lower opening is installed at the high permeable zone, the water volume flow to the wellbore will decrease.

The following three cases were simulated to see the effects of change of pressure drop across the valve and minimum opening at the closed position. The simulated cases are presented in Table 5-5.

Table 5-5: Simulated cases for different AICD parameters

10%	Wells with AICDs having relative opening of 10% when it is in closed position (Diameter – 20 mm, CD – 0.84)
5%	Wells with AICDs having lower minimum opening (5%) at the high permeable zone and 10% minimum opening in the rest of the zones (All AICDs with diameter = 20 mm, CD = 0.84)
10% res	Wells with an AICD with relatively high flow restriction at the high permeable zone (*Diameter – 0.2mm*) and normal AICDs in the rest of the zones (Diameter – 20 mm, CD – 0.84), All AICDs with minimum opening of 10%

The accumulated oil and water for these cases are presented in Figure 5-23. The water accumulation with non-uniform AICD is the lowest among all the simulated model. Thus, the reduction of valve diameter is more effective than the reduction of the minimum opening of the valve at the high permeable zone. The reduction of the minimum opening from 10% to 5% of the valve at high permeable zone does not have so much influence on the oil accumulation. This is due to the fact that the oil volume flow is comparatively low compared to water volume flow in the later part of the production. The accumulated oil volume decreased with the higher pressure drop across the valve.

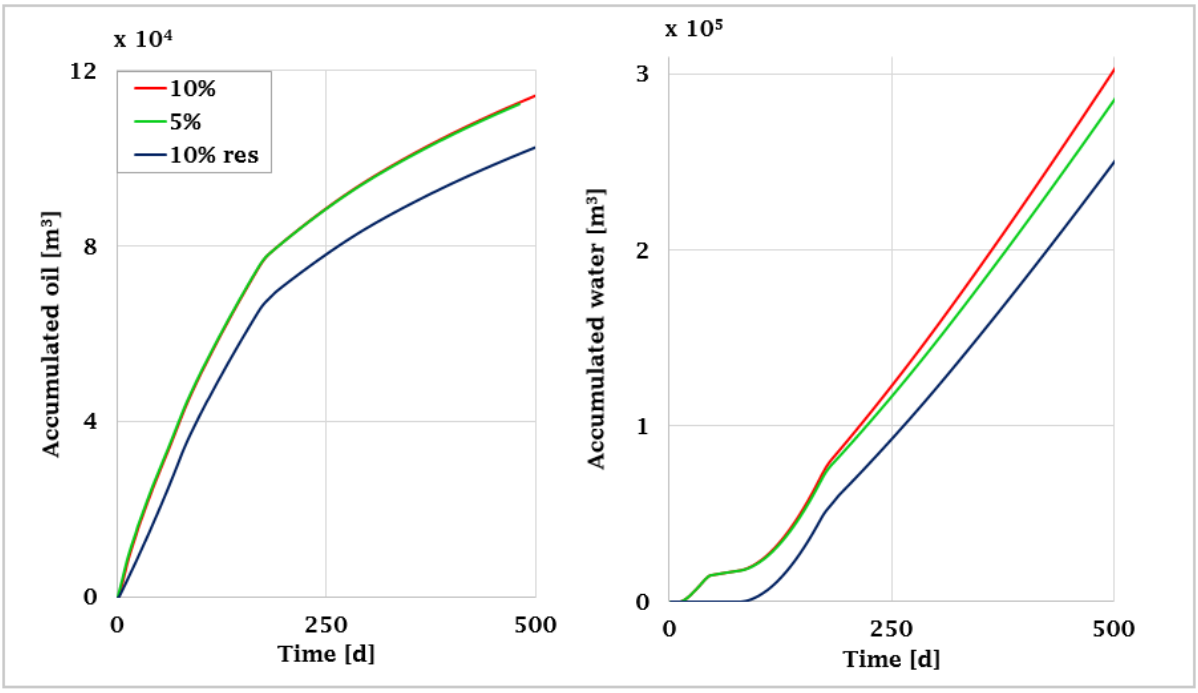

Figure 5-23: Accumulated oil and water for different AICD parameters_1

To get higher oil production, a new model was simulated with the increase of minimum opening of AICD in all of the low permeable zones. The additional case is presented in Table 5-6.

Table 5-6: Additional case

5%, rest 12%	Wells with an AICD having lower minimum opening (5%) at the high permeable zone and other AICDs with 12% minimum opening in the rest of the zones (Diameter – 20 mm, CD – 0.84)

Figure 5-24 shows the accumulated oil and water profile. The new combination has produced a higher amount of oils but also the water accumulation has increased. Therefore, the acceptable minimum opening and the pressure drop across the valve have to decide based on the types of application.

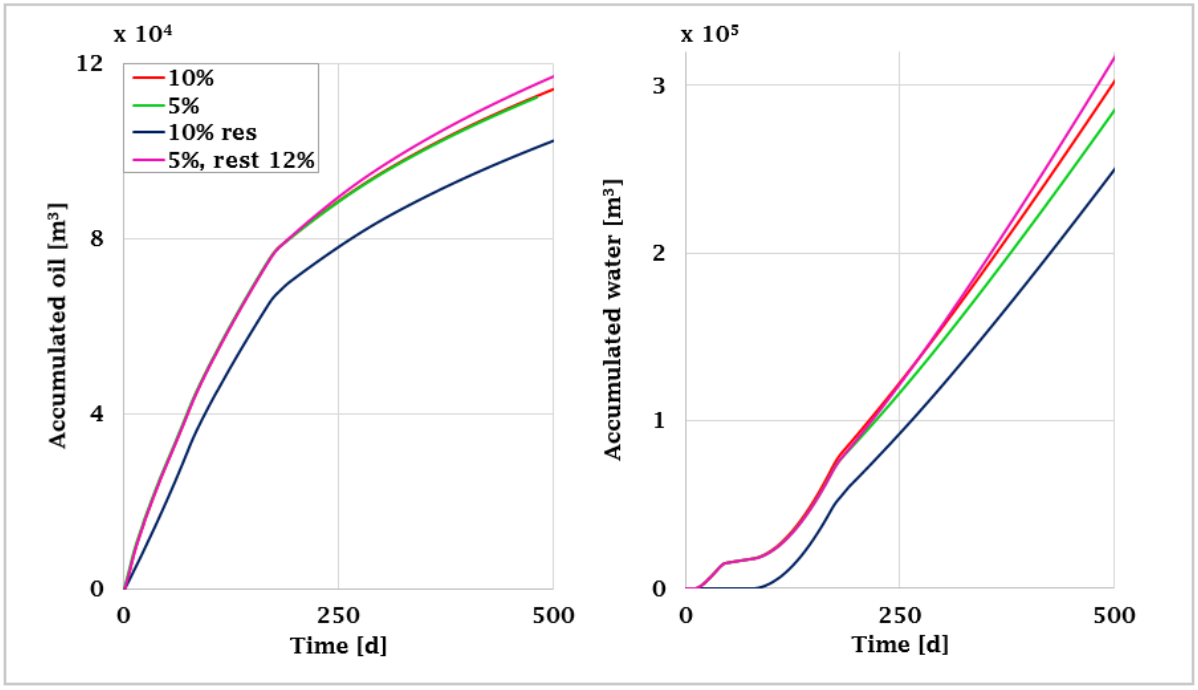

Figure 5-24: Accumulated oil and water for different AICD parameters_2

5.5 Equivalent vs non-equivalent

Generally, all the above simulations were based on the equivalent AICD which represents 8 AICDs for simplicity. In practice, a well consists of an AICD installed per a length of 12.4 m of well. In this analysis, the effects of considering such an equivalent valve were studied and analyzed. A separate model was developed which represents just two zones, one with relatively low permeability (1000 mD) and the other with relatively high permeability (10000 mD). Since

the Rocx module was unable to represent more than 20 zones for the heterogeneous reservoir. Figure 5-25 shows the model for this simulation. The equivalent case contains an equivalent valve in both zone, whereas the non-equivalent case contains normal 16 valves throughout the two zones.

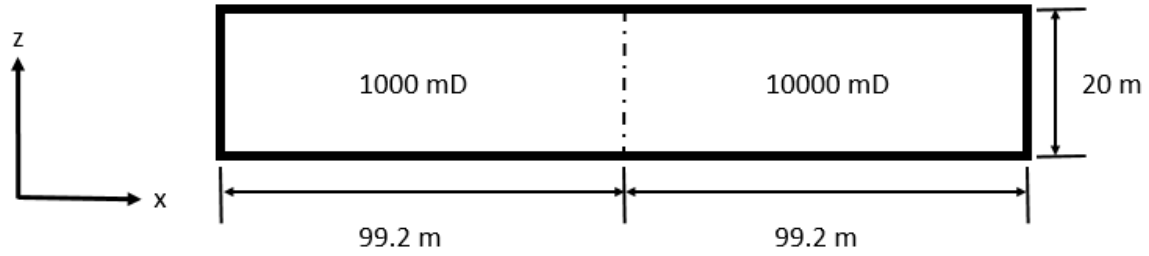

Figure 5-25: Reservoir for equivalent vs non-equivalent case in xz plane

It would be interesting to see the results with this consideration. As expected, there would be some difference between these two modes, as the equivalent model does not necessarily represent the exact model.

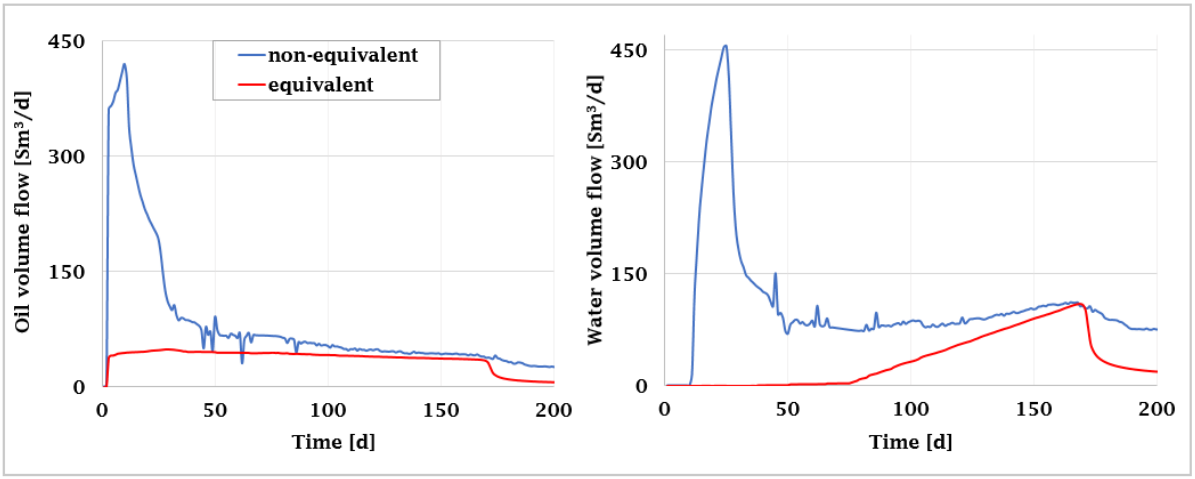

Figure 5-26: Liquid flow rates

Figure 5-26 represents the accumulated oil and oil volume flow at standard conditions for the above-discussed cases with light oil. The oil production rate decreased significantly for the non-equivalent case as soon as the water breakthrough had occurred. The water volume flow before the closure of autonomous devices is quite high for non-equivalent case compared to the equivalent case. The early liquid production is dominated by production from high permeability zone. Hence, the high water volume flow is due to the combined flow rate of eight valve compared to one valve in high permeability zone. Further, water breakthrough has been delayed with the consideration of equivalent model.

The equivalent case has only one equivalent AICD in each of the zones, so the oil production rate is low compared to the non-equivalent case. The reason for this difference in oil volume flow can be illustrated in Figure 5-27.

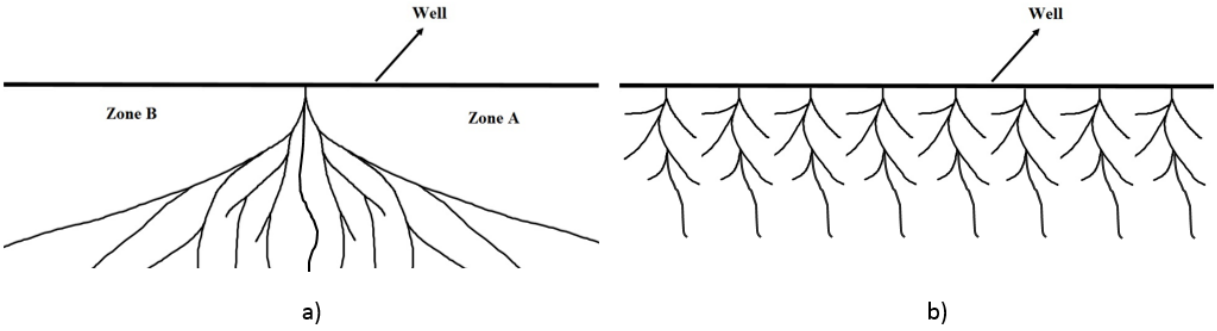

Figure 5-27: Fluid drainage patterns for: - a): equivalent b): non-equivalent case

The fluids for the case of the equivalent case has to travel a long distance compared to that of non-equivalent cases. They prefer to move straight to the inflow opening, which creates a significant amount of non-active zones like zone A and zone B as shown in Figure 5-27 (a). This makes difficult for the oil to go into the valve opening from those inactive zones. For the non-equivalent case, the inactive zones are much smaller compared to that of the equivalent zone. Hence, the oil production with the help of equivalent AICD gives less than that of normal AICD. Of course, installing more normal AICD quite closer to each other won't be the ideal solution because of their cost. Therefore, the optimal length between two AICDs installations must be determined considering all these aspects. This shows that the equivalent model can predict the reservoir-wellbore behavior but not able to produce the exactly same results.

5.6 Discussion

The water accumulation increases continuously with the use uniform ICD for all types of reservoirs. High water flow rates during the oil production reduce the oil flow rates. Further, oil production with a high amount of water requires large water separation systems adding the operational cost of the plants. Oil containing a higher amount of water increases the corrosion rates of the plants, which reduces the lifetime of the well. Therefore, AICD and the non-uniform ICD are simulated as an alternative to the uniform ICD system.

From the obtained results, it can be said that AICDs is better inflow controller to limit the water influx into the wellbore. They are more effective in heterogeneous and fractured reservoirs compared to the homogeneous reservoir. Once the AICD closes, both the oil and water flow rates will reduce. As a result, the accumulated oil from the mature oil fields will reduce. AICDs take more than 20 days to reach a fully closed position from the fully open position, resulting in higher production of water.

If it is possible to locate the fractured zones inside the reservoir, then from the simulation results of the case with relatively high flow restriction in the high permeable zone, early water breakthrough is delayed. But, it is challenging to find the precise location of the high permeable zones. The restrictive ICD will reduce the oil production if installed in zones other than the high permeable zones. So, there would be high risk installing restrictive inflow controllers.

For a constant relative permeability of oil and water, the oil volume flow increases with the decrease of oil viscosity. This is due to the increase of mobility of oil. The mobility of oil increases with the decrease of mobility ratio and mobility ratio decreases with the decrease of

oil viscosity. The flow rate with doubling the size of mesh was comparatively the same as with the normal mesh size in the x-direction. The flow rate is almost the same except at the time of closure of AICD. The finer grid shows the more accurate behavior during the closing of AICD.

The pressure drop across the valve and the allowable flow area at the closed positions are the design parameters of AICD. The pressure drop across the valve can be changed by changing the valve diameter. The production rates decrease by increasing the restriction of the flow, resulting in less accumulation of oil and water. The flow area of AICD in closed positions affects the oil and water accumulation in the system. The higher the flow area in closed positions, the higher will the accumulated volumes be.

An equivalent AICD was chosen to represent eight normal AICDs to make the simulation more efficient in terms of both time and computational resources. Additional simulations were performed by using normal sized AICDs, and the results show that the liquid volume flow is high compared to the results obtained using the equivalent AICDs. The oil production with the non-equivalent AICD has more uniformly distributed inflow profile across the wellbore than that of the equivalent case. The non-active zones near to the well with equivalent AICDs results in higher residual oil in the reservoir.

6 Conclusion

During this work, the near-well simulations have been done for light and heavy oil reservoirs. The behavior of the fractured, heterogeneous and homogeneous reservoirs is studied with normal ICDs, non-uniform ICDs and AICDs. Early water breakthrough occurred due to the fractures or the heterogeneity in the reservoirs. The water breakthrough from the fractured, heterogeneous and homogenous light oil reservoirs is observed after 9, 25 and 75 days of production respectively. The same pattern is observed with heavy oil.

The non-uniform ICDs has the ability to delay the early water breakthrough. The restriction introduced on an ICD at the high permeable zone of the light oil reservoir is able to delay the initial water breakthrough from day 9 to day 76. The main drawback of this case is the high installation risks as it is difficult to pre-locate the fractured zones inside a reservoir.

The frictional pressure drop along the well is around 0.1 bar for homogeneous reservoir causing almost same production in all zones of the well. The water breakthrough occurred at about same time along the whole well and all the AICDs closed during a short time interval. Therefore, the effects of AICDs are less significant in the homogeneous reservoir.
From the above simulations results, water accumulation can be reduced by the use of AICDs or the non-uniform ICDs. After a specified amount of water associated with the flow, AICD choked the total flow entering the wellbore. AICDs are better to limit the water accumulation and the water production was reduced with 88% compared to the normal ICDs in the heterogeneous light oil reservoir. The water accumulation in the fractured light oil reservoir reduced significantly by around 82% and oil accumulation by 29% by the use of AICD compared to normal ICDs. The production from the high permeability zones is choked locally by using AICDs, allowing normal oil production from the other zones. Therefore, AICDs are better suited for heterogeneous and fractured reservoirs.
The oil volume flow increased with the decrease of oil viscosity. This is due to the higher mobility of oil. For the same relative permeability, there is around 47% increase in oil flow rate with the decrease of oil viscosity from 3 cP to 1.5 cP and 120 % increase in oil flow rate with the decrease of oil viscosity from 3 cP to 0.8 cP after 10 days. The oil volume flow and water volume flow are almost the same with doubling the number of the grid along the well. Thus, confirming that the developed model is nearly insensitive to the mesh sizes in the well direction.

The restriction can be minimized with a higher minimum opening at the closed position. This will in turn increases the water influx into the wellbore. The results show that 10% minimum opening at the closed position has 6% more accumulated water compared to 5% minimum opening at a closed position in the high permeable zone. The results show that with a more restrictive valve in the high permeable zone, the accumulated oil reduced by almost 10% and the accumulated water reduced by 17%. Thus, the reasonable opening at the closed position and valve diameter have to be decided based on the application.

The use of equivalent valves in the simulations gives less oil volume flow compared to the normal valves. This observation is of significant importance for further work.

To get a proper performance of the autonomous devices, proper tuning of the PID controller should be done and studied further. The obtained results should be validated experimentally to implement the developed model in real practice

7 References

[1] A. Malagalage, "Near well simulation and modelling of oil production from heavy oil reservoirs," Høgskolen i Telemark, 2015.

[2] O. A. Alomair and A. S. Almusallam, "Heavy crude oil viscosity reduction and the impact of asphaltene precipitation," *Energy & Fuels,* vol. 27, no. 12, pp. 7267-7276, 2013.

[3] (27.02.2017). *API Graavity*. Available: http://www.petroleum.co.uk/api

[4] (27.02.2017). *Light Crude Oil*. Available: https://sites.google.com/site/aboutcrudeoil/light-crude-oil

[5] P. Fernandes, Z. Li, and D. Zhu, "Understanding the roles of inflow-control devices in optimizing horizontal-well performance," in *SPE Annual Technical Conference and Exhibition*, 2009: Society of Petroleum Engineers.

[6] H.-E. B. Torbergsen, "Application and design of passive inflow control devices on the Eni Goliat oil producer wells," University of Stavanger, Norway, 2010.

[7] V. Birchenko, K. Muradov, and D. Davies, "Reduction of the horizontal well's heel–toe effect with inflow control devices," *Journal of Petroleum Science and Engineering*, vol. 75, no. 1, pp. 244-250, 2010.

[8] F. T. Al-Khelaiwi, V. M. Birchenko, M. R. Konopczynski, and D. Davies, "Advanced wells: a comprehensive approach to the selection between passive and active inflow-control completions," *SPE Production & Operations*, vol. 25, no. 03, pp. 305-326, 2010.

[9] M. Halvorsen, G. Elseth, and O. M. Nævdal, "Increased oil production at Troll by autonomous inflow control with RCP valves," in *SPE Annual Technical Conference and Exhibition*, 2012: Society of Petroleum Engineers.

[10] R. C. Selley and S. A. Sonnenberg, *Elements of petroleum geology*. Academic Press, 2014.

[11] P. Inc. *Oil and Gas Fundamentals,* . Available: http://mpgpetroleum.com/fundamentals.html

[12] M. Economides, A. Hill, and C. Ehlig-Economides, "Petroleum production systems," 1994.

[13] D. Hatzignatiou and F. Mohamed, "Water and gas coning in horizontal and vertical wells," in *Annual Technical Meeting*, 1994: Petroleum Society of Canada.

[14] V. Mathiesen, B. Werswick, and H. Aakre, "The next generation inflow control, the next step to increase oil recovery on the Norwegian continental shelf," in *SPE Bergen One Day Seminar*, 2014: Society of Petroleum Engineers.

[15] T. Ahmed, *Reservoir engineering handbook*. Gulf Professional Publishing, 2006.

[16] J. Lasater, "Bubble point pressure correlation," *Journal of Petroleum Technology*, vol. 10, no. 05, pp. 65-67, 1958.

[17] J. J. Velarde, "Correlation of black oil properties at pressures below the bubble-point," Texas A&M University, 1996.

8 Appendices

Appendix A: Thesis task description

University College of Southeast Norway

Faculty of Technology, Natural Sciences and Maritime Sciences, Campus Porsgrunn

FMH606 Master's Thesis

Title: Near-well simulations and modelling of oil production from reservoir

USN supervisor: Britt Moldestad

External partner: Acona Flow Technology

Co- supervisor: Rune Killie, Acona Flow Technology

Task background:
Near-well simulations have previously been performed and published for a heavy-oil reservoir, and the resulting accumulated oil production was compared for different inflow control technologies. The main objective of this master's thesis will be to repeat the simulations with light instead of heavy oil and with a different type of inflow control technology. Various sensitivity simulations will be required in order to evaluate the robustness of the results.

Task description:

The work will consist of the following main activities:

- Go through and understand previously performed work.
- Reproduce at least one simulation result.
- Go through the existing simulation model together with external partner in order to fully understand all modelling assumptions and input values.
- Repeat the previously performed simulations, but with different oil properties, and compare the results.
- In the previous simulation work, eight valves were combined into one equivalent valve for simplicity. Simulate the effect of *not* combining valves.
- Repeat the previous simulation, but with the reservoir section tilted downward, such that water separates and accumulates in the lower part of each annulus zone.
- Include a realistic well profile and simulate the overall effect on the wells productivity.

Student category: PT. The student need to have good knowledge about oil production, reservoir and near well simulation.

Practical arrangements:
Necessary software will be provided by TUC

Signatures:

Student (date and signature):

Supervisor (date and signature): Britt Moldestad

Address: Kjølnes ring 56, NO-3918 Porsgrunn, Norway. **Phone:** 35 57 50 00. **Fax:** 35 55 75 47.

Appendix B: Lasater correlation [17]

Bubble point pressure

$$P_b = \frac{0.2268 \cdot 10^{(4.258 y_g)}(T + 459.67)}{\gamma_g} \text{ (for } \gamma_g \leq 0.7) \quad (8.1)$$

$$P_b = \frac{(8.26 y_g^{3.56} + 1.95)(T + 459.67)}{\gamma_g} \text{ (for } \gamma_g \geq 0.7) \quad (8.2)$$

Separator gas mole fraction

$$y_g = \frac{R_{sb}/379.3}{R_{sb}/379.3 + 350 \cdot \gamma_o / M_o} \quad (8.3)$$

Effective oil molecular weight

$$M_o = 630 - 10 \cdot \gamma_{API} \text{ (for API} \leq 40) \quad (8.4)$$

$$M_o = 73110 \cdot \gamma_{API}^{-1.562} \text{ (for API} \geq 40) \quad (8.5)$$

Solution gas oil ratio

$$R_{sb} = \frac{132755 \cdot \gamma_o \cdot y_g}{M_o(1 - y_g)} \quad (8.6)$$

Bubble point pressure factor

$$p_f = \frac{p_b \cdot \gamma_g}{(T + 459.67)} \quad (8.7)$$

Separator gas mole fraction

$$y_g = \frac{\ln\left(\frac{p_f}{0.2268}\right)}{4.258} \text{ (for } p_f \leq 5) \quad (8.8)$$

$$y_g = \left(\frac{p_f - 1.95}{8.26}\right)^{0.2809} \text{ (for } p_f \geq 5) \quad (8.9)$$

The range of data used to develop this Lasater correlation are presented below: -

Table A: Data range used in lasater correlation

Range	Units
48 < P_b < 5780	Psia
82 < T < 272	°F
3 < R_{sb} < 2905	scf/STB
17.9° < API < 51.1°	°API
0.574 < γ_g < 1.223	(air = 1)

Appendix C: Reservoir model in Rocx (light oil)

```
#  Version: 1.2.5.0
#  Input file created by Input File Editor.
#  4/29/2017 9:07:41 PM


*GEOMETRY RECTANGULAR

#  Number of grid blocks in horizontal and vertical direction
#  ----------------------------------------------------------
#  nx   ny   nz
   10   29   10

   dx   const   99.2
   dy   j   3.5   3.5   3.5   3.5   3.5   3   3   3   2.5   2.5   2.5   2   2   1.5   1   1.5   2   2   2.5   2.5
   2.5   3   3   3   3.5   3.5   3.5   3.5   3.5
   dz   const   2

#  Direction vector for gravity
#  ----------------------------
#  gx   gy   gz
   0   0   1

*FLUID_PARAMETERS

   blackoil

#  Black oil option data
#  ---------------------
   gormodel   Lasater
   massfrac

   rsgo_bp_tuning off

   oilvisc_tuning on

   gor   150
   gasspecificgravity   0.64
   oilspecificgravity   0.85
   oilvisc   3
   visctemp   100
   viscpress   130

#  Black oil component data
#  ------------------------
   ncomp   3

   label   BO_Oil_0
   type   oil
   oilspecificgravity   0.92

   label   BO_Gas_0
   type   gas
   gasspecificgravity   0.64
   h2smolefraction   1E-06
   co2molefraction   1E-06
   n2molefraction   1E-06

   label   BO_Water_0
   type   water
```

```
   waterspecificgravity    1


#  Black oil feed data
#  -------------------
   nfeed    2

   label    Feed_3
   oilcomponent    BO_Oil_0
   gascomponent    BO_Gas_0
   gor    150

   watercomponent    BO_Water_0
   watercut    0.0001
   label    Feed_1
   oilcomponent    BO_Oil_0
   gascomponent    BO_Gas_0
   glr    0.0001

   watercomponent    BO_Water_0
   watercut    0.99

*RESERVOIR_PARAMETERS

#  Permeability (mDarcy) in principal directions
#  ---------------------------------------------
   permx    ijk
  1000    1000    1000    10000    1000    1000    1000    1000    1000    1000
  -       -       -       -        -       -       -       -       -       -

   permy    ijk
  1000    1000    1000    10000    1000    1000    1000    1000    1000    1000
  -       -       -       -        -       -       -       -       -       -

   permz    ijk
  100    100    100    1000    100    100    100    100    100    100
  -      -      -      -       -      -      -      -      -      -

#  Porosity
#  --------
   por    const    0.3

#              compr    reference_pressure
   rock_compr    0    0



#  swc    sor    sgr
   0    0    0

   krw
   0.1    0
   0.11    0.003
   0.12    0.005
   0.15    0.013
   0.2    0.025
   0.25    0.038
   0.3    0.05
   0.35    0.082
```

0.4 0.114
0.45 0.145
0.5 0.177
0.55 0.233
0.6 0.289
0.65 0.344
0.7 0.4
0.75 0.48
0.8 0.56
0.85 0.64
0.9 0.72
0.95 0.86
1 1 /

kro
0.1 0
0.11 0.003
0.12 0.005
0.15 0.013
0.2 0.025
0.25 0.038
0.3 0.05
0.35 0.082
0.4 0.114
0.45 0.145
0.5 0.177
0.55 0.233
0.6 0.289
0.65 0.344
0.7 0.4
0.75 0.48
0.8 0.56
0.85 0.64
0.9 0.72
0.95 0.86
1 1 /

krg
0.1 0
0.11 0.003
0.12 0.005
0.15 0.013
0.2 0.025
0.25 0.038
0.3 0.05
0.35 0.082
0.4 0.114
0.45 0.145
0.5 0.177
0.55 0.233
0.6 0.289
0.65 0.344
0.7 0.4
0.75 0.48
0.8 0.56
0.85 0.64
0.9 0.72
0.95 0.86
1 1 /

Pcow

```
   0   1
   1   0   /

   Pcgo
   0   0
   1   1   /

*BOUNDARY_CONDITIONS

manual

#  Injection flow rates
#  --------------------
#  nsource
   0

#  ix   iy   iz   ntime   time   mw   mo   mg   temp

#  Production pressures
#  --------------------
#  npres_bou
   11

#  i   j   k   idir   type   name   ntime   time   pres_bou   temp_bou   Sw_bou   So_bou   Sg_bou
Feeds
   1-10   1-29   10   3   res   Water_drive   1   0   130   100   1   0   0   [Feed_1 1]
#  i   j   k   idir   type   rw   name   ntime   time   skin   WIFoil   WIFgas   WIFwater   pres_bou
temp_bou   Sw_bou   So_bou   Sg_bou
   10   15   3   1   well   0.1   P10   1   0   0   1   1   1   130   100   0   1   0   [Feed_3 1]
   9   15   3   1   well   0.1   P9   1   0   0   1   1   1   130   100   0   1   0   [Feed_3 1]
   8   15   3   1   well   0.1   P8   1   0   0   1   1   1   130   100   0   1   0   [Feed_3 1]
   7   15   3   1   well   0.1   P7   1   0   0   1   1   1   130   100   0   1   0   [Feed_3 1]
   6   15   3   1   well   0.1   P6   1   0   0   1   1   1   130   100   0   1   0   [Feed_3 1]
   5   15   3   1   well   0.1   P5   1   0   0   1   1   1   130   100   0   1   0   [Feed_3 1]
   4   15   3   1   well   0.1   P4   1   0   0   1   1   1   130   100   0   1   0   [Feed_3 1]
   3   15   3   1   well   0.1   P3   1   0   0   1   1   1   130   100   0   1   0   [Feed_3 1]
   2   15   3   1   well   0.1   P2   1   0   0   1   1   1   130   100   0   1   0   [Feed_3 1]
   1   15   3   1   well   0.1   P1   1   0   0   1   1   1   130   100   0   1   0   [Feed_3 1]

*INITIAL_CONDITIONS

#  Feed
   feed const [Feed_3 1] /

manual

#  Saturations
#  -----------
   sw   const   0
   so   const   1
   sg   const   0

#  Pressures
#  ---------
   Po   const   130

#  Temperatures
#  ------------
   T   const   100

*TEMPERATURE off
```

```
*INTEGRATION

#  tstart    tstop
   0    0

#  dtmin    dtmax    dtstart    dtfac    cflfac
   100    3600    0.01    10    1

implicit Linsolver

*WELL_COUPLING_LEVEL
   4

*OUTPUT

#  cof_time    cof_rate
   1    1

#  ntplot
   10
   P10
   P9
   P8
   P7
   P6
   P5
   P4
   P3
   P2
   P1

   Dt_Trend
   0    3600    /

   Dt_Prof
   0    3600    /

   screen_info    1

*END
```

Appendix D: Wellbore model in OLGA

1. Introduction

Project	OLGA
Case description	Basic Case
Date	
Author	Schlumberger

2. Simulation Options

Overall setting	Flow model	OLGA
	Mass eq scheme	1STORDER
	Compositional model	BLACKOIL
	Debug	OFF
	Drilling	
	Phase	THREE
	Elastic walls	OFF
	Void in slug	SINTEF
	Steady state	OFF
	User defined plug-in	OFF
	Temp. calc.	OFF
	Wax deposition	
	Restart	OFF
Integration	Simulation starttime	0 s
	Simulation stoptime	1200 d
	Minimum time step	100 s
	Maximum time step	3600 s

3. System Layout - Graphics

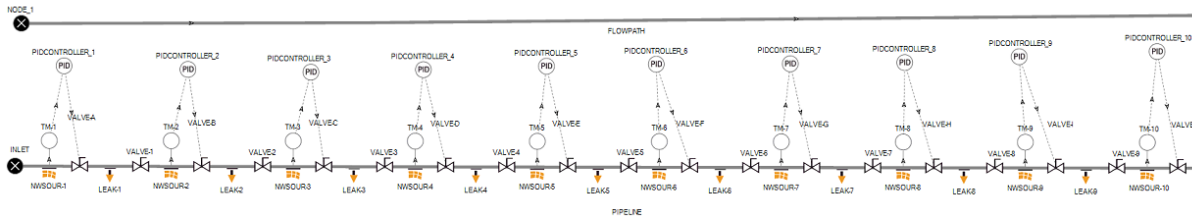

4. System Layout - Table

4.1 Summary

4.1.1 Overall

No. of Branches	No. of Pipes	No. of Sections

2	2	60

4.1.2 Flows

Branches	No. of Pipes	No. of Sections	Min. Section Length	At	Max. Section Length	At
PIPELINE	1	20	49.6 M	PIPE-1	49.6 M	PIPE-1
FLOWPATH	1	20	49.6 M	PIPE-1	49.6 M	PIPE-1

4.2 Layout

Pipe no.	Branch	Label	Diameter	Roughness	XEnd	YEND	Wall
1 - 1	PIPELINE	PIPE-1	0.1 M	2.8E-05 M	992 M	0 M	WALL-1
2 - 1	FLOWPATH	PIPE-1	0.1 M	5E-05 M	992 M	0 M	WALL-1

5. Insulation and Walls

5. 1 Material

Label	Density	Conductivity	Heat Capacity
MATER-1	7850 kg/m3	50 W/m-C	500 J/kg-C
MATER-2	2500 kg/m3	1 W/m-C	880 J/kg-C

5. 2 Walls

Label	Material	Wall thickness	Elastic
WALL-1	MATER-1	0.009 m	
	MATER-2	0.02 m	
	MATER-2	0.02 m	
WALL-2	MATER-1	0.0075 m	
	MATER-2	0.02 m	
	MATER-2	0.02 m	

6. Boundary Conditions

6. 1 Nodes

Label	Type	Pressure	Temperature
INLET	CLOSED		
OUTLET	CLOSED		

NODE_1	CLOSED		
OUTPUT	PRESSURE	120 bara	100 C

6. 2 Initial Conditions

Branch	Pipe	Mass Flow	VoidFraction	WaterCut
PIPELINE	ALL	0	0 -	0
FLOWPATH	ALL	0	0 -	0

7. Equipment

7. 1 Valves

Label	Branch	Pipe	Section	Diameter	Opening	CD
VALVE-A	PIPELINE	PIPE-1	2	0.02 m	1	0.84
VALVE-1	PIPELINE	PIPE-1	3	0.1 m	0	0.84
VALVE-B	PIPELINE	PIPE-1	4	0.02 m	1	0.84
VALVE-2	PIPELINE	PIPE-1	5	0.1 m	0	0.84
VALVE-C	PIPELINE	PIPE-1	6	0.02 m	1	0.84
VALVE-3	PIPELINE	PIPE-1	7	0.1 m	0	0.84
VALVE-D	PIPELINE	PIPE-1	8	0.02 m	1	0.84
VALVE-4	PIPELINE	PIPE-1	9	0.1 m	0	0.84
VALVE-E	PIPELINE	PIPE-1	10	0.02 m	1	0.84
VALVE-5	PIPELINE	PIPE-1	11	0.1 m	0	0.84
VALVE-F	PIPELINE	PIPE-1	12	0.02 m	1	0.84
VALVE-6	PIPELINE	PIPE-1	13	0.1 m	0	0.84
VALVE-G	PIPELINE	PIPE-1	14	0.02 m	1	0.84
VALVE-7	PIPELINE	PIPE-1	15	0.1 m	0	0.84
VALVE-H	PIPELINE	PIPE-1	16	0.02 m	1	0.84
VALVE-8	PIPELINE	PIPE-1	17	0.1 m	0	0.84
VALVE-I	PIPELINE	PIPE-1	18	0.02 m	1	0.84
VALVE-9	PIPELINE	PIPE-1	19	0.1 m	0	0.84
VALVE-J	PIPELINE	PIPE-1	20	0.02 m	1	0.84

7. 2 Position

Label	Branch	Pipe	Section
POS-1	FLOWPATH	PIPE-1	2
POS-2	FLOWPATH	PIPE-1	4
POS-3	FLOWPATH	PIPE-1	6
POS-4	FLOWPATH	PIPE-1	8
POS-5	FLOWPATH	PIPE-1	10
POS-6	FLOWPATH	PIPE-1	12
POS-7	FLOWPATH	PIPE-1	14
POS-8	FLOWPATH	PIPE-1	16
POS-9	FLOWPATH	PIPE-1	18
POS-10	FLOWPATH	PIPE-1	20